

# NAVAL POSTGRADUATE SCHOOL

## Monterey, California



## THESIS

**ANALYSIS AND MODELING OF THE ACOUSTIC  
TOMOGRAPHY SIGNAL TRANSMISSION FROM  
DAVIDSON SEAMOUNT TO SUR RIDGE:  
THE FORWARD PROBLEM**

by

Jose Alberto de Mesquita Onofre

September 1999

Thesis Advisor:

Ching-Sang Chiu

Co-Advisor:

Curtis A. Collins

Approved for public release; distribution is unlimited.

20000424 152

<b>REPORT DOCUMENTATION PAGE</b>			Form Approved OMB No. 0704-0188	
Public reporting burden for this collection of information is estimated to average 1 hour per response, including the time for reviewing instruction, searching existing data sources, gathering and maintaining the data needed, and completing and reviewing the collection of information. Send comments regarding this burden estimate or any other aspect of this collection of information, including suggestions for reducing this burden, to Washington headquarters Services, Directorate for Information Operations and Reports, 1215 Jefferson Davis Highway, Suite 1204, Arlington, VA 22202-4302, and to the Office of Management and Budget, Paperwork Reduction Project (0704-0188) Washington DC 20503.				
1. AGENCY USE ONLY (Leave blank)		2. REPORT DATE September 1999		3. REPORT TYPE AND DATES COVERED Master's Thesis
4. TITLE AND SUBTITLE ANALYSIS AND MODELING OF THE ACOUSTIC TOMOGRAPHIC SIGNAL TRASMISSION FROM DAVIDSON SEAMOUNT TO SUR RIDGE: THE FORWARD PROBLEM			5. FUNDING NUMBERS	
6. AUTHOR(S) Jose Alberto de Mesquita Onofre				
7. PERFORMING ORGANIZATION NAME(S) AND ADDRESS(ES) Naval Postgraduate School Monterey, CA 93943-5000			8. PERFORMING ORGANIZATION REPORT NUMBER	
9. SPONSORING / MONITORING AGENCY NAME(S) AND ADDRESS(ES)			10. SPONSORING / MONITORING AGENCY REPORT NUMBER	
11. SUPPLEMENTARY NOTES The views expressed in this thesis are those of the author and do not reflect the official policy or position of the Department of Defense or the U.S. Government.				
12a. DISTRIBUTION / AVAILABILITY STATEMENT Approved for public release; distribution is unlimited.			12b. DISTRIBUTION CODE	
13. ABSTRACT (maximum 200 words)  The repeated transmissions of a tomography signal from an autonomous sound source placed on Davidson Seamount was continuously monitored by a bottom-lying, cabled-to-shore receiver on Sur Ridge. To address the signal stability, resolvability and identifiability criteria that determine the applicability of ocean tomography along this path, the data recorded from July 1998 to January 1999 were first processed to obtain the multipath pulse arrival structure and its variability in time. The processed signals showed strong arrivals that were both stable and resolvable. In order to identify the resolved arrivals, acoustic propagation modeling was performed using ray theory in conjunction with measured sound speed and high-resolution bathymetric data. A comparison of the predicted and measured arrival structures show that the observed arrivals were clearly identifiable and were made up of eigenray groups (i.e., eigenray tubes) instead of individual eigenrays. Since the eigenrays within each group were found to have almost identical trajectories through the ocean, the common passage along which the ray group integrates the ocean variability was unambiguous. Consistent with previous CalCOFI observations, the extracted ray group travel time series exhibited dominant oscillations with semidiurnal, diurnal, 8-day, 18-day and 26-day periods, respectively. Using spectral estimation techniques, the travel time variances of these dominant oscillations were quantified. These travel time variances represent direct measurements of the variances of spatially averaged ocean temperatures. Therefore, they are useful for establishing the solution and noise variances for the construction of the inverse solution as well as constituting a powerful statistical data set for the validation of ocean models for the region.				
14. SUBJECT TERMS Tomography, Oceanography, Monterey Bay, ICON			15. NUMBER OF PAGES 53	
			16. PRICE CODE	
17. SECURITY CLASSIFICATION OF REPORT Unclassified	18. SECURITY CLASSIFICATION OF THIS PAGE Unclassified	19. SECURITY CLASSIFICATION OF ABSTRACT Unclassified	20. LIMITATION OF ABSTRACT UL	



Approved for public release; distribution is unlimited.

**ANALYSIS AND MODELING OF THE ACOUSTIC TOMOGRAPHY  
SIGNAL TRANSMISSION FROM DAVIDSON SEAMOUNT TO  
SUR RIDGE: THE FORWARD PROBLEM**

Jose Alberto de Mesquita Onofre  
Lieutenant, Portuguese Navy  
B.S., Portuguese Naval Academy, 1992

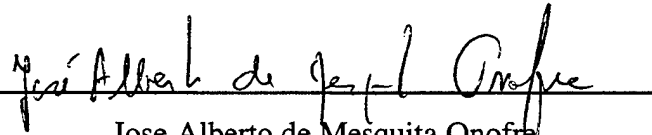
Submitted in partial fulfillment of the  
requirements for the degree of

**MASTER OF SCIENCE IN PHYSICAL OCEANOGRAPHY**


from the

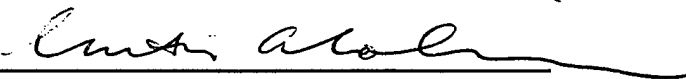
**NAVAL POSTGRADUATE SCHOOL  
September 1999**

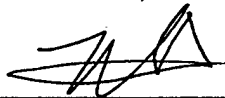
Author:

  
Jose Alberto de Mesquita Onofre

Approved by:

  
Ching-Sang Chiu, Thesis Advisor

  
Curtis A. Collins, Co-Advisor

  
Roland W. Garwood Jr., Chairman  
Department of Oceanography



## ABSTRACT

The repeated transmissions of a tomography signal from an autonomous sound source placed on Davidson Seamount was continuously monitored by a bottom-lying, cabled-to-shore receiver on Sur Ridge. To address the signal stability, resolvability and identifiability criteria that determine the applicability of ocean tomography along this path, the data recorded from July 1998 to January 1999 were first processed to obtain the multipath pulse arrival structure and its variability in time. The processed signals showed strong arrivals that were both stable and resolvable. In order to identify the resolved arrivals, acoustic propagation modeling was performed using ray theory in conjunction with measured sound speed and high-resolution bathymetric data. A comparison of the predicted and measured arrival structures show that the observed arrivals were clearly identifiable and were made up of eigenray groups (i.e., eigenray tubes) instead of individual eigenrays. Since the eigenrays within each group were found to have almost identical trajectories through the ocean, the common passage along which the ray group integrates the ocean variability was unambiguous. Consistent with previous CalCOFI observations, the extracted ray group travel time series exhibited dominant oscillations with semidiurnal, diurnal, 8-day, 18-day and 26-day periods, respectively. Using spectral estimation techniques, the travel time variances of these dominant oscillations were quantified. These travel time variances represent direct measurements of the variances of spatially averaged ocean temperatures. Therefore, they are useful for establishing the solution and noise variances for the construction of the inverse solution as well as constituting a powerful statistical data set for the validation of ocean models for the region.



## TABLE OF CONTENTS

<b>I.</b>	<b>INTRODUCTION.....</b>	<b>1</b>
A.	COASTAL OCEANOGRAPHY OF CENTRAL CALIFORNIA .....	1
B.	THE INNOVATIVE COASTAL-OCEAN OBSERVING NETWORK .....	2
C.	ACOUSTIC TOMOGRAPHY .....	3
D.	THESIS OBJECTIVES .....	4
E.	THESIS OUTLINE .....	5
<b>II.</b>	<b>OBSERVATIONS.....</b>	<b>7</b>
A.	ACOUSTIC DATA .....	7
1.	The Experiment .....	7
2.	Sound Transmission Recording .....	9
3.	Arrival Structure – 1000 Hz Sampling Rate .....	11
4.	Arrival Structure – 2000 Hz Sampling Rate .....	14
5.	Findings on Stability and Resolvability .....	15
B.	OCEANOGRAPHIC DATA .....	17
1.	R.V. “ <i>Point Sur</i> ” Cruise .....	17
2.	Moored Temperature Data .....	18
<b>III.</b>	<b>MODELING .....</b>	<b>21</b>
A.	ARRIVAL STRUCTURE SYNTHESIS .....	21
B.	RAY IDENTIFICATION .....	26
<b>IV.</b>	<b>VARIABILITY .....</b>	<b>31</b>
A.	POWER SPECTRAL DENSITY OF TRAVEL TIME .....	31
B.	VARIANCE DISTRIBUTION .....	34
<b>V.</b>	<b>CONCLUSIONS.....</b>	<b>37</b>
	<b>LIST OF REFERENCES .....</b>	<b>39</b>
	<b>INITIAL DISTRIBUTION LIST .....</b>	<b>41</b>





## ACKNOWLEDGMENTS

I would like to thank Professor Ching-Sang Chiu, my advisor, for stimulation in the subject, for informative discussions and mostly for a never ending supply of encouragement, especially when my work seemed to lead to nowhere in particular. Without his direction and availability for discussions, I certainly would have run about in circles. Without him, this thesis would not have been possible.

Special thanks goes to Chris Miller, to whom I owe a great deal. His guidance and expertise in the data analysis and processing played an integral role in my learning of the subject area as well as provided me with the necessary detail for my work with acoustic tomography.

I would also like to thank Professor Curtis Collins for his assistance and expertise in explaining the oceanography of the Central California coast to me as well as provided me useful suggestions for thesis writing, and Rob Bourke for keeping the computers running and helping me solving the numerous programming errors that I made during this work.

Finally, I wish to thank my wife Ana for her patience and support. Without her I could have not completed my studies at Naval Postgraduate School.



## **I. INTRODUCTION**

### **A. COASTAL OCEANOGRAPHY OF CENTRAL CALIFORNIA**

The Central California coastal oceanography is characterized by complex features due to several different environmental conditions affecting the ocean. Upwelling is a very common occurrence along the California coast during summer. The atmospheric pressure field in the Pacific induces Northerly winds bringing to the surface cold water with a significant impact in the thermocline and mixed layer structure. Coastal circulation during the upwelling season is highly variable and difficult to quantify, being driven primarily by the local wind field.

As traditionally defined, the California current flows equatorward year round. It is strongest at the sea surface and generally extends over the upper 500 m of the water column carrying cold, fresh subarctic water equatorward along the coast (Hickey, 1998).

The California undercurrent flows poleward over the continental slope from Baja California to close proximity of Vancouver Island, transporting warmer, saltier water poleward along the coast (Wooster and Jones, 1970; Hickey, 1979; Chelton, 1984; Rosenfeld et al., 1994; Tisch et al., 1992). Peak speeds of the undercurrent are about 30-50 cm s<sup>-1</sup> being stronger at depths of 100-300 m and can be continuous over distances of more than 400 km along the slope (Collins et al., 1996).

The Davidson current flows poleward in fall and winter from Point Conception to beyond Vancouver Island. It has been suggested that the Davidson current is the result of the "surfacing" of the California Undercurrent during fall (Pavlova, 1966; Huyer and

Smith, 1974). Measurements in the region have shown that the seasonal cycle over the slope is highly variable with the poleward flow maximum usually occurring in May (Collins et al., 1996)..

This complex coastal circulation system, consisting of multiple, variable currents, mesoscale eddies, and upwelling activities, exhibits significant variability from synoptic to interannual scales. Thus, in order to develop a predictive capability, it is apparent that a long-term, coastal observing network with sufficient resolution to allow for gaining fundamental insights into the detailed physics is required.

## **B. THE INNOVATIVE COASTAL-OCEAN OBSERVING NETWORK**

Under the sponsorship of the National Ocean Partnership Program (NOPP), an alliance was formed between government, academia and private industry to implement an Innovative Coastal-Ocean Observing Network (ICON) to study the oceanography in the Central California coastal waters surrounding the Monterey Bay (Paduan et al., 1999). Marine scientists and engineers collaborating in this research project, called ICON, come from eight different organizations including the Naval Postgraduate School (NPS), Monterey Bay Aquarium Research Institute (MBARI), California State University at Monterey Bay (CSUMB), University of Southern Mississippi (USM), University of Michigan (UM), HOBI Labs, CODAR Ocean Sensors Ltd. (COS), and Naval Research Laboratory (NRL). The goals of ICON are to employ a suite of complimentary, near real-time coastal ocean instrumentations to measure the critical ocean parameters, and to

assimilate these measurements into predictive models for the purpose of forecasting coastal ocean conditions.

The principal instruments in ICON include shore-based, remote-sensing high-frequency (HF) radars, in situ, realtime temperature, salinity and current sensors, and acoustic tomography. The acoustic tomography component consists of two autonomous sound sources, one placed on Davidson Seamount and the other on Pioneer Seamount. The acoustic transmissions are monitored continuously by a receiver lying on Sur Ridge. The data are brought back to shore by the NPS Ocean Acoustic Observatory (OAO) at Pt Sur via an underwater cable in real time.

### **C. ACOUSTIC TOMOGRAPHY**

Exploiting the physical characteristics of how ocean sound propagates from a fixed source to a fixed receiver, tomography integrates the sound-speed variations along the many different eigenrays and stores the information in the multipath travel times of the transmitted signal (Munk et al., 1995). Since sound speed changes are caused mainly by temperature changes and because the transmission loss of low-frequency sound is relatively low, tomography can rapidly (i.e., almost instantaneously) sample ocean temperature variability over large distances. Additionally, repeated transmissions of the same signal over an extended period of time can yield long-term, high-resolution time series.

The purpose of the tomography element in ICON is to provide acoustic travel-time data that directly measure path-averaged temperature changes and maps of

temperature variability along the two acoustic slices through data inversion. While mapping the temperature changes in both space and time is relevant to ocean process studies, the statistics of path-averaged temperatures represent unique data for validating and calibrating predictive ocean models.

However, high-quality travel time data series and inverse maps can only be attained providing that the received signals possess stable, resolvable and identifiable arrivals. Stable arrivals are those that show up consistently in repeated transmissions over an extended period of time. Adjacent arrivals in the same transmission are resolved if they don't overlap. Arrivals are identified if the measured arrival structure resembles the predicted arrival structure such that the measured arrivals can be associated with the different paths of propagation. When positive identification of stable, resolved arrivals is achieved, accurate path-integral relations between the travel time data and unknown temperature (or sound-speed) variations are established. This is known as solving the forward problem of tomography. The inverse solution is often constructed as a minimum mean-square-error estimate with specified (a priori) solution and noise variances (Cornuelle et al., 1983, and Chiu et al. 1994).

#### **D. THESIS OBJECTIVES**

Different from an open-ocean application of regional tomography, the realization of stable, resolvable and identifiable arrivals in a coastal ocean is not always guaranteed. This is due to the existence of more irregular acoustic multipaths resulting from a fully or partially bottom-limited, range-dependent propagation condition. Because of this reason,

the measured signals from the ICON tomography component warrant a careful, systematic investigation into the stability, resolvability and identifiability issues of the forward problem. Such an investigation is the thrust of this thesis. The focus is on the Davidson Seamount-to-Sur Ridge transmissions. The sound source on Davidson Seamount was deployed first and the corresponding transmission has produced a sufficiently long data record to permit a forward analysis.

Thus, the overall objective of this study is to solve the forward problem of tomography that is associated with the Davidson Seamount-to-Sur Ridge transmission path. This includes:

1. The investigation of whether stable and resolvable arrivals exist.
2. The identification of the propagation paths of stable, resolved arrivals.
3. The validation of the quality of the extracted series of travel times of the arrivals.
4. The quantification of the distribution of the variances of the dominant ocean time scales as observed in the acoustic travel times.

## **E. THESIS OUTLINE**

To accomplish the objectives of this study, each of the signals received in a six-month period, from 14 July 1998 to 12 January 1999, were first processed (i.e., pulse compressed and ensemble averaged) to give the multipath arrival structure of a pulse with a high signal-to-noise ratio. Arrival peaks of the repeated transmissions were then extracted (i.e., picked) to facilitate a visual analysis of stability and resolvability. The



identification process involved comparing data to a model prediction. The modeling used a range-dependent, Hamiltonian raytracing code developed by Jones et al. (1986), in conjunction with external eigenray-search and waveform-synthesis algorithms documented in Morvillez (1997). The input environmental model for the raytracing was developed based on measured hydrographic data and high-resolution bathymetric data. Moored oceanographic data were used to validate the quality of the acoustic travel time data, and a spectral analysis was performed to study the observed ocean variability.

The experimental geometry, acoustic data, findings on stability and resolvability, and oceanographic data used to support quality check and propagation modeling are presented in Chapter II. The propagation modeling and ray identification results are discussed in Chapter III. Results from the variability analysis are discussed in Chapter IV, and conclusions are given in Chapter V.

## II. OBSERVATIONS

### A. ACOUSTIC DATA

#### 1. The Experiment

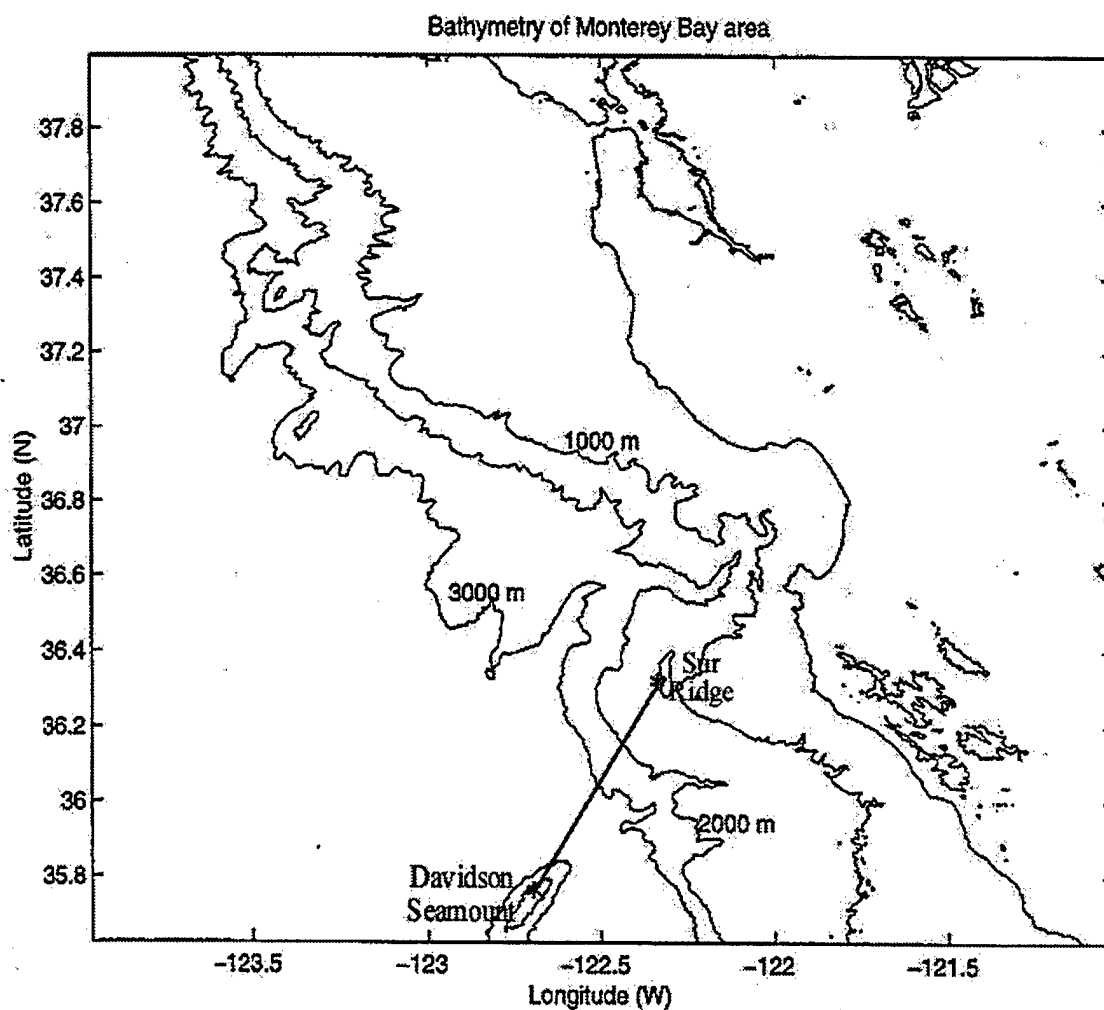


**Fig. 1 – The orientation of the Davidson Seamount-to-Sur Ridge acoustic path along with the regional bathymetry.**

The orientation of the acoustic path along with the surrounding bathymetry are shown in Fig. 1. The transmitter is located on Davidson Seamount at a depth of 1270 m. It has a source level of 183 dB re 1 $\mu$ Pa, center frequency of 400 Hz, and bandwidth of

100 Hz. It has been transmitting phase-modulated tomography signals periodically since July 1998. The signals were recorded at the Point Sur OAO with a cabled-to-shore receiver located on Sur Ridge. The receiver is lying on the bottom at a depth of 1359 m. The acoustic track is only 65 km long, over variable bathymetry, presenting a good challenge for the application of tomography techniques.

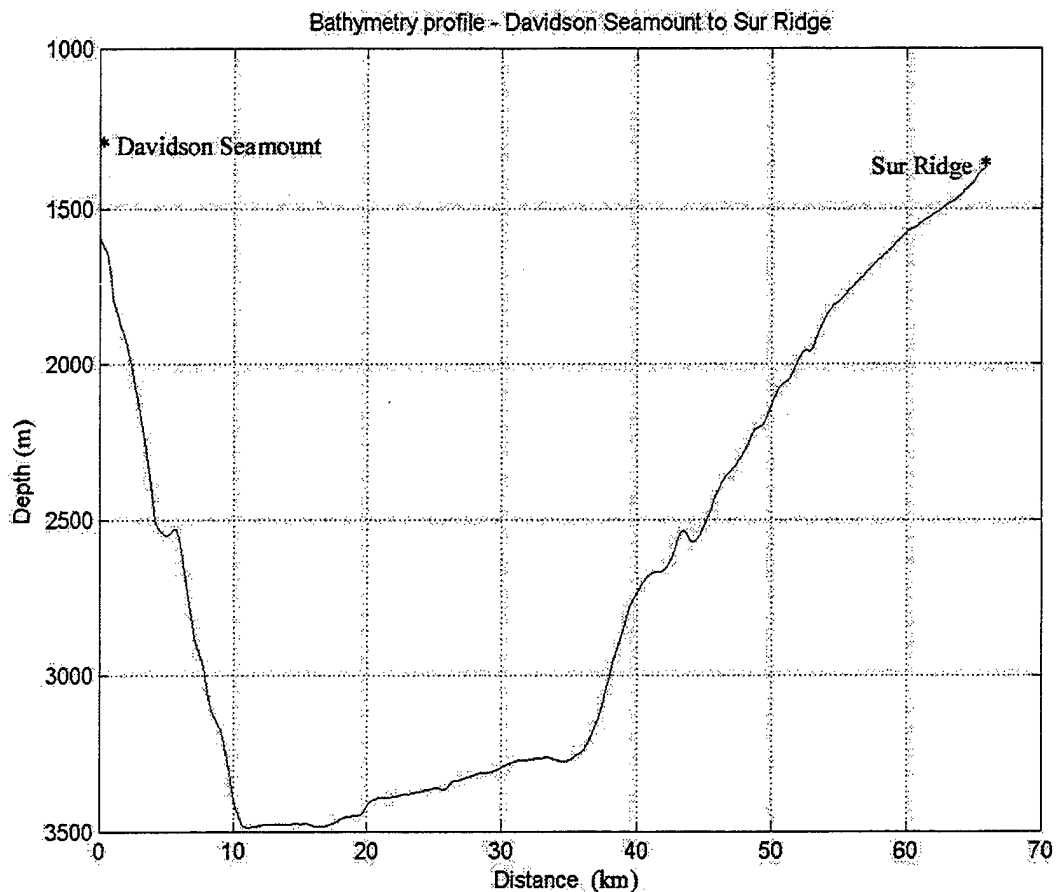


**Fig. 2 - Bathymetry profile along the transmission path**

Multipath acoustic arrivals in shorter ranges are generally less spread in time and, hence, may not be resolvable with a single, omni-directional hydrophone. Identifying the

arrivals with particular ray paths may also become more difficult in this case. This is because the inevitable bottom interactions with the slopes near the source and receiver could introduce ray chaos in the approximate ray theory (model). The highly variable bathymetry along the acoustic path is shown in Fig. 2, clearly presenting a partially bottom-limited propagation condition. This bathymetry was interpolated from a 250-m resolution data set provided by the United States Geological Survey (USGS), Menlo Park, California, and was used in the acoustic modeling.

## **2. Sound Transmission Recording**

By design, the battery-powered sound source was programmed to transmit tomography signals with two different repetition rates, every 30 min in the first month, from 30 July to 28 August of 1998, and then switched to every 12 hrs to cover an extended period, with the objective to resolve both tidal and longer-term variability. The tidal signal variance is important in that it constitutes an important “noise” component in monitoring the longer scales, and thus needs to be quantified. The signals were also recorded with two different sampling rates at the Point Sur OAO. The every-30-min initial transmissions were sampled at a rate of 1000 Hz, whereas the subsequent every-12-hrs transmissions were sampled at 2000 Hz. Only data collected between 30 July 1998 and 12 January were analyzed in this study. The analyzed data consist of 1106 and 272 repeated transmissions from 30 July 1998 to 28 August 1998, and from 29 August 1998 to 12 January 1999, respectively.

The time synchronization at the receiver was provided by Network Time Protocol (NTP). There were some technical problems with the collection of the data, resulting in

the presence of data gaps in the time-series. These problems are documented in Table 1. The source timing was referenced to Global Positioning System (GPS) prior to deployment. After the source is recovered, the source clock will be compared to GPS time again to determine clock drift. Clock drift errors will be compensated to improve the precision of the measurements of acoustic travel time.

On 12 January 1999, a telecommunications outage caused the unclassified (single-hydrophone) data acquisition computer at the OAO to lose synchronization to GPS time. This occurrence introduced irregular timing errors that are not readily correctable. The problem was detected and solved in early June but has shortened the time-series for the present study.

<b>Data Outage (day/time)</b>	<b>Length</b>	<b>Reason for outage</b>
1998 YearDay 225-226	27.6 hours	Loss of building power, no auto-restart
1998 YearDay 226-231	119.3 hours	Loss of building power, no auto-restart
1998 YearDay 281-282	1.98 hours	System maintenance
1998 YearDay 284-286	40.92 hours	Data unrecoverable
1998 YearDay 306-307	26.9 hours	Disk storage 100% full
1998 YearDay 318-321	72.1 hours	Disk storage 100% full
1998 YearDay 364-365	39.3 hours	Data link broken, unable to remote backup files
1999 YearDay 12-147	135 days	Telephone cable cut by construction work. Absolute timing of single phone data is questionable from this point due to CPU drift of workstation

**Table 1 – Technical problems affecting data continuity.**

### **3. Arrival Structure – 1000 Hz Sampling Rate**

All sound tracks were processed with a correlation matched filter. The output corresponds to the sum of pulses, arriving from the multiple eigenrays. Each pulse has a duration of approximately 10 ms. Since 35 sequences with a period of 5.11 s were transmitted every time, ensemble averaging to further improve the signal-to-noise ratio (SNR) is possible.

From 30 July 1998 to 28 August of 1998, a transmission was made every 30 min and was recorded with a sampling rate of 1000 Hz at the OAO. Although slightly above the theoretical Nyquist criterion, this sampling rate was determined, empirically, to be insufficient to produce an improved SNR through coherent averaging of the sequences. An aliasing effect, corresponding to the introduction of a frequency-independent phase roll in the digitized signal, was found. This phase roll would cause severe signal degradation, if the sequences were averaged coherently. This degradation is illustrated in Fig. 3, where a severely low SNR is observed.

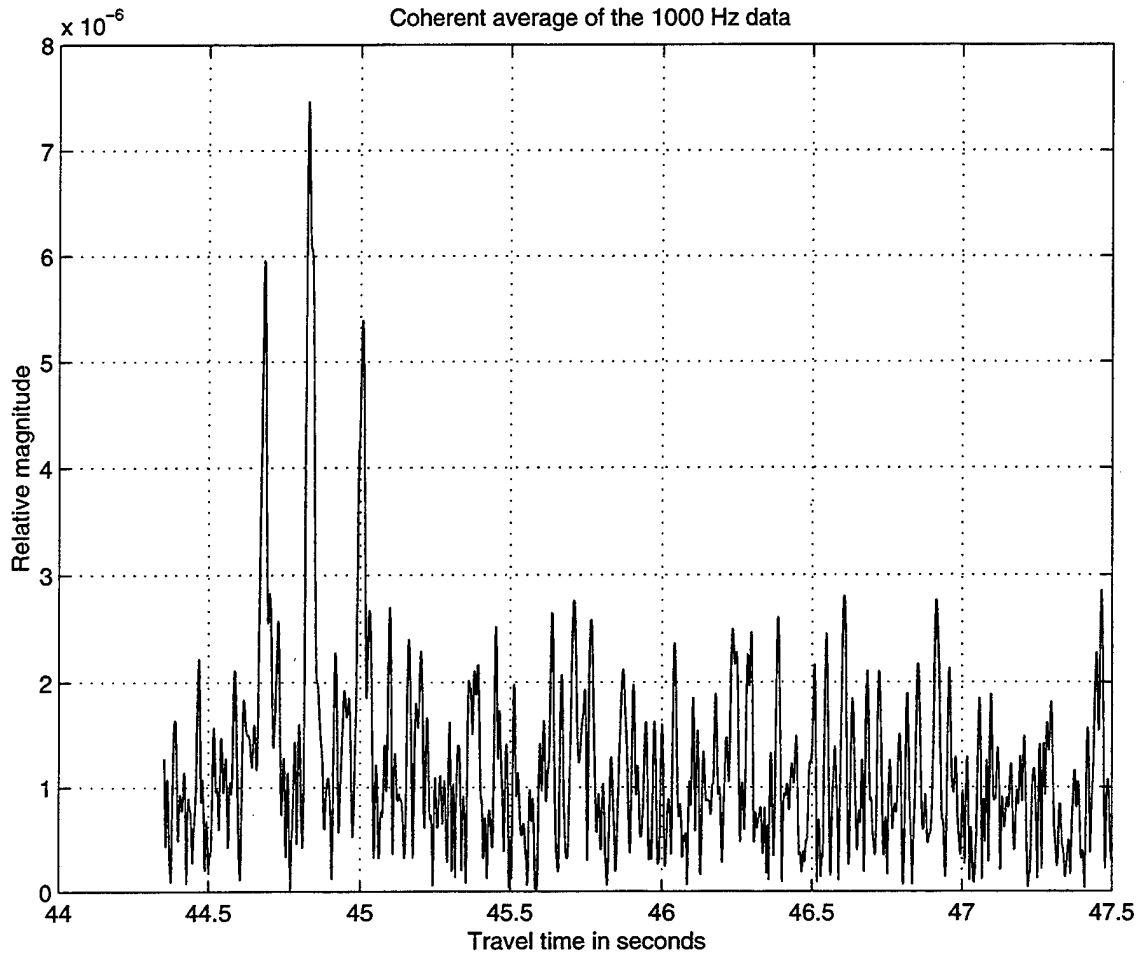


**Fig. 3 – Example result of a coherent average of signals sampled at 1000 Hz**

A remedy is to perform incoherent averaging instead. Using incoherent averaging, a high enough SNR was achieved. An example of the incoherently averaged result is displayed in Fig. 4, showing a clean multipath arrival structure of 2.5-s long above the noise background.

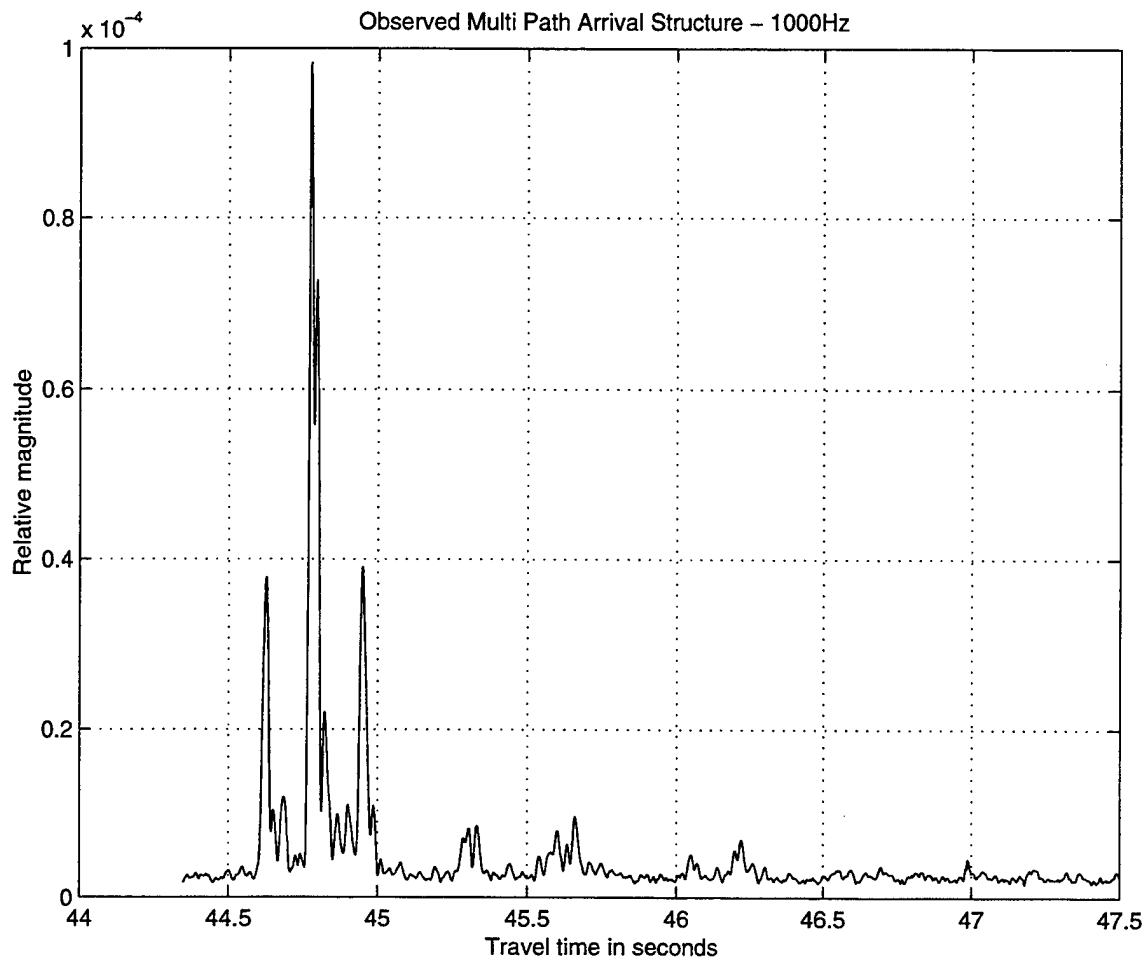


**Fig. 4 – Example result of an incoherent average of signals sampled at 1000 Hz**

After processing all the transmissions sampled with the 1000 Hz rate, the travel times of all arrival peaks exceeding a threshold were extracted. The results are displayed in Fig. 5 as a dot plot, useful for an examination of the stability and resolvability of the arrivals.

The extraction of the arrival peaks was not fully automated. A program developed by Chris Miller, Manager of the NPS OAO, was used to extract the travel times of all the



peaks exceeding a noise estimate in a window. The window moves in time with its center following a path controlled by the operator.

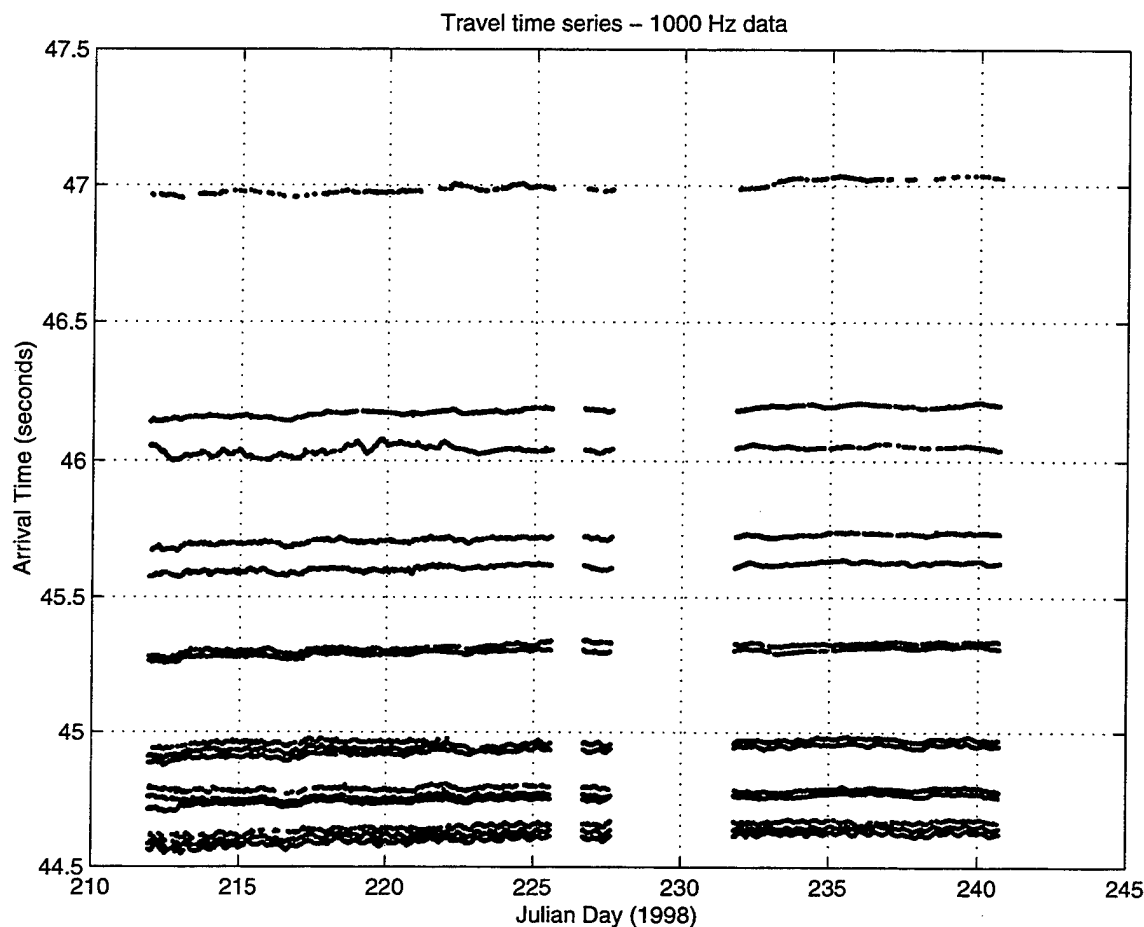


**Fig. 5 – Dot plot of travel times of acoustic arrivals from 30 July 1998 to 28 August of 1998**

#### **4. Arrival Structure – 2000 Hz Sampling Rate**

From 29 August 1998 to 12 January 1999, the sampling rate was doubled, i.e., changed to 2000 Hz. This has avoided any aliasing effects and made coherent averaging highly desirable. An example of the coherently averaged results is shown in Fig. 6. The processed arrival structure is seen to closely resemble those derived from incoherent

averages (Fig. 4.), but with a much reduced noise background. Using the same technique as before, the multipath travel times of the acoustic arrivals in this time period were extracted. The results are displayed in Fig. 7, again as a dot plot. Gaps in both dot plots correspond to periods where no data exist due to the technical problems described in Table 1.

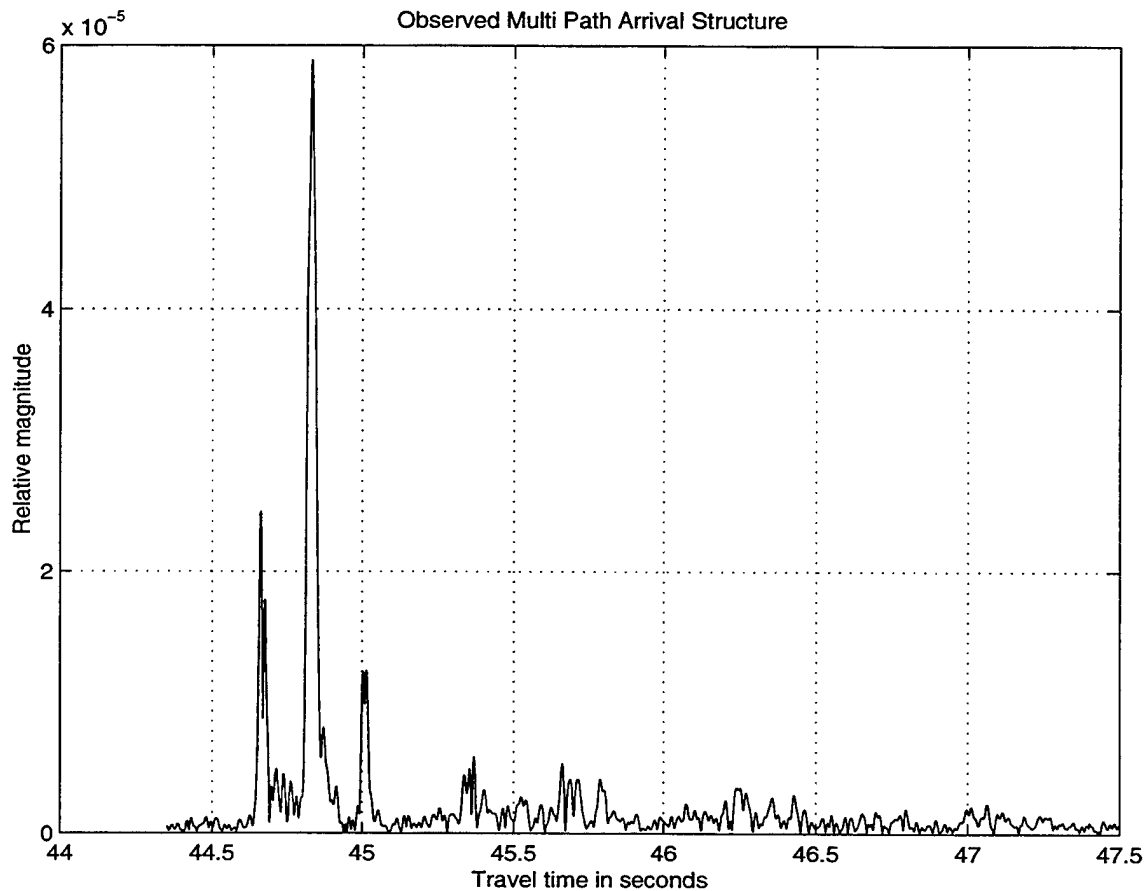


**Fig. 6 – Example result of a coherent average of signals sampled at 2000 Hz**

### **5. Findings on Stability and Resolvability**

As a whole, both Figs. 5 and 7 show distinctive traces of dots, each representing a stable, resolved arrival. Exceptions are found, however, in the second and third groups of three, counting from the beginning. The second group of three arrivals merged into two

on approximately Julian Day (JD) 230, 1998, and then changed back to three on approximately JD 250, 1998. The third group of three merged into two on approximately JD 223, 1998, and stayed as a group of two for the remaining period. These two groups represent stable but marginally resolved arrivals. The remaining 10 arrivals, however, are both stable and resolvable.

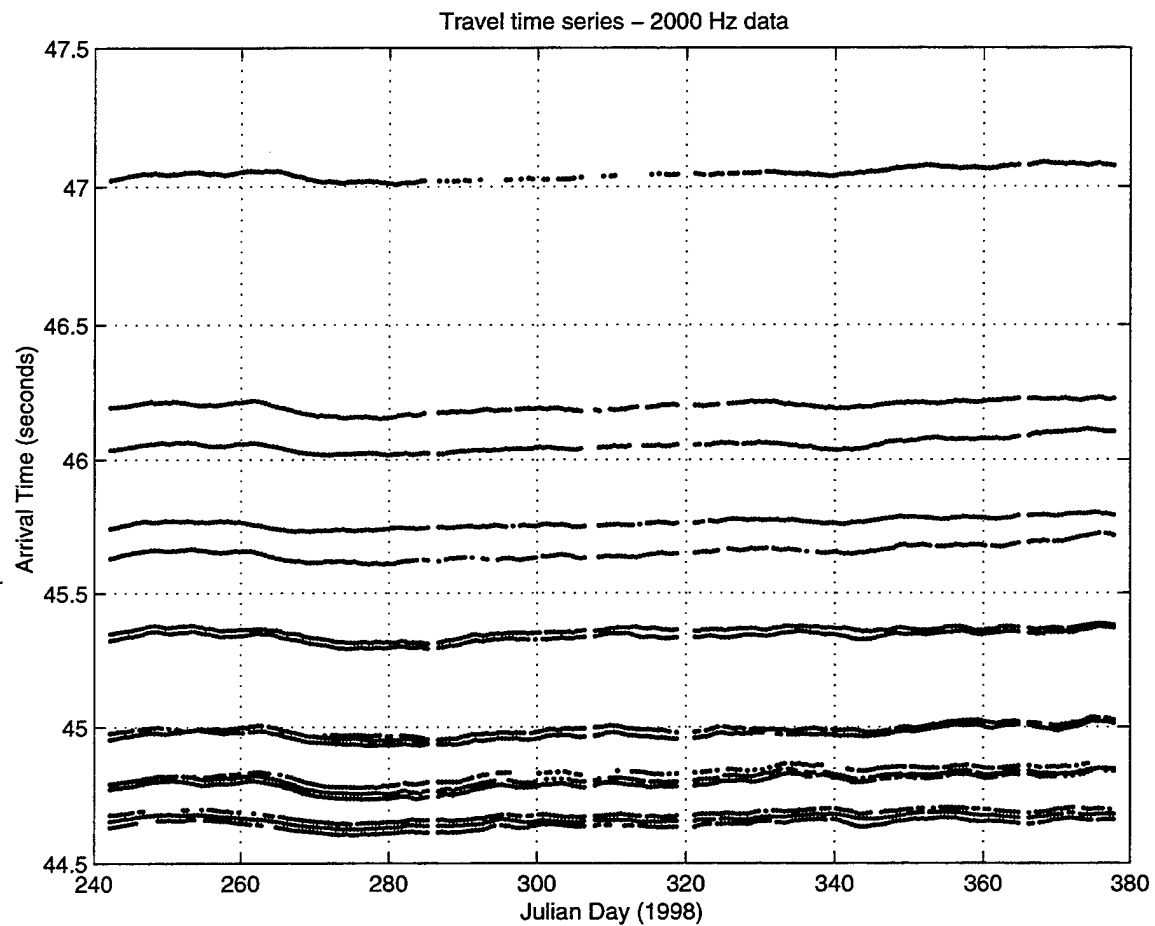


**Fig. 7 - Dot plot of travel times of acoustic arrivals from 29 August 1998 to 12 January 1999.**

## B. OCEANOGRAPHIC DATA

### 1. R.V. "Point Sur" Cruise

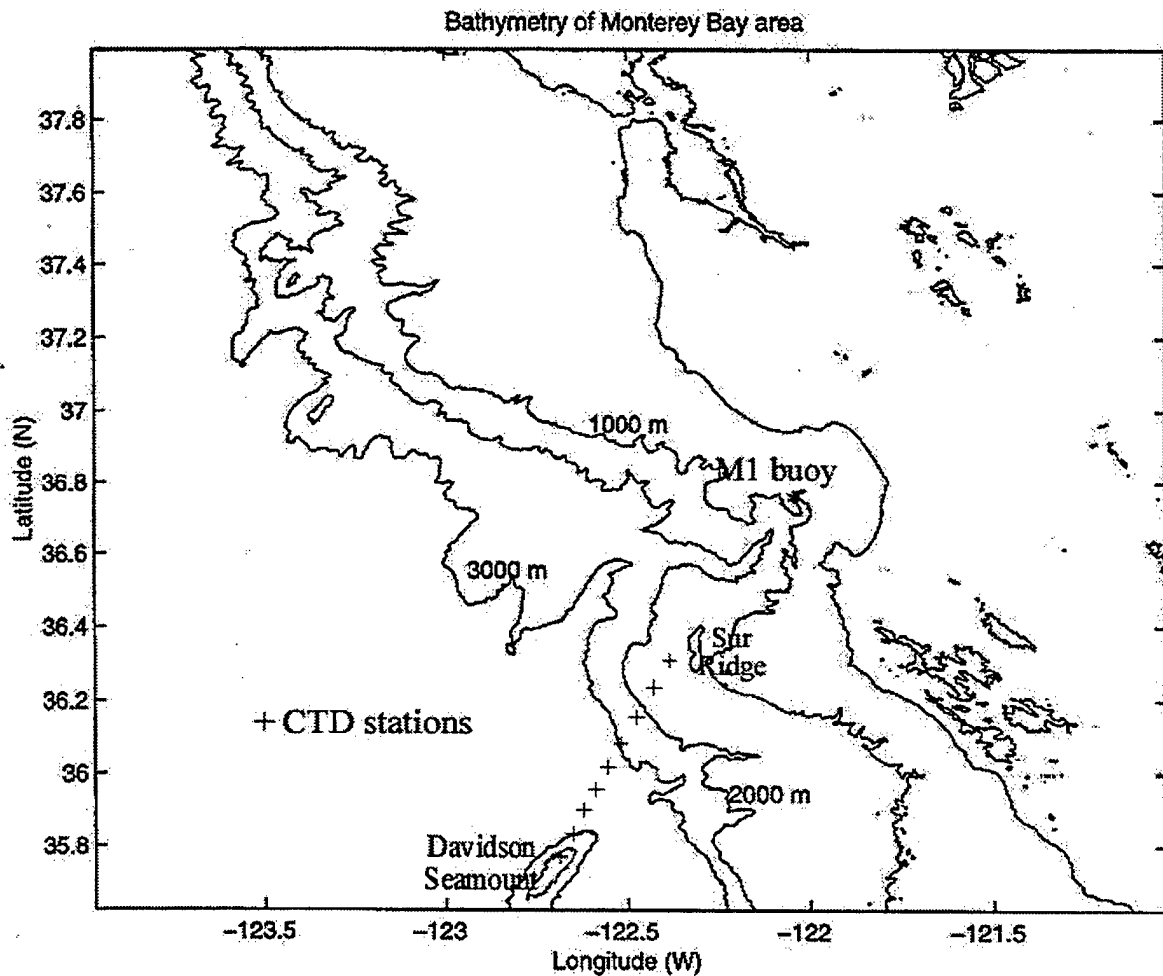


**Fig. 8 – Locations of the CTD stations performed along the acoustic transmission path**

A 1998 summer cruise of the R.V. "Point Sur" provided CTD data from 9 stations between Davidson Seamount and Sur Ridge. To establish the "reference" ocean for the acoustic modeling, sound speed was computed based on temperature, salinity and pressure information from each station. Since the resultant sound speed profiles exhibit only small differences, it is appropriate to assume that the reference ocean has a range-

independent sound-speed field defined as the range average of the nine profiles. To prevent numerical instability in the model runs, the sound speed profile for the reference ocean was further filtered to remove any sharp gradients, i.e., fine structure. This reference sound speed profile is shown in Fig. 9.

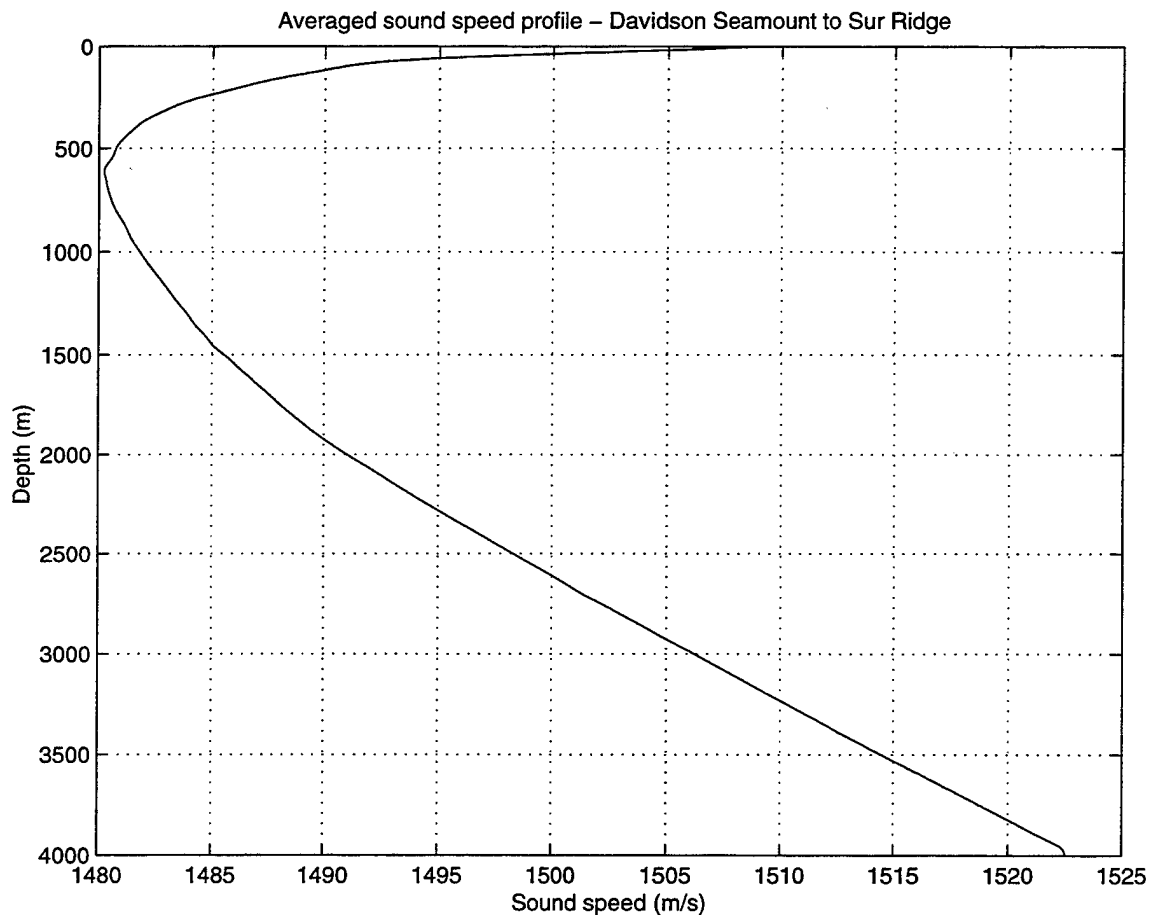


**Fig. 9 - Averaged and filtered sound speed profile used for acoustic modeling**

## **2. Moored Temperature Data**

An oceanographic mooring, deployed by the Monterey Bay Aquarium Research Institute (MBARI), has provided an *in situ* temperature time-series covering the same period as the acoustic transmissions. This temperature time-series is shown in Fig. 10 as

nine curves denoting measured temperature at nine different depths, 20, 40, 60, 80, 100, 150, 200, 250 and 300 m, respectively. Labeled as M1, the location of this MBARI mooring is shown in Figure 8. In spite of not being close to the acoustic path, regional events as observed by M1 can be used to validate the quality of the acoustic travel time data.

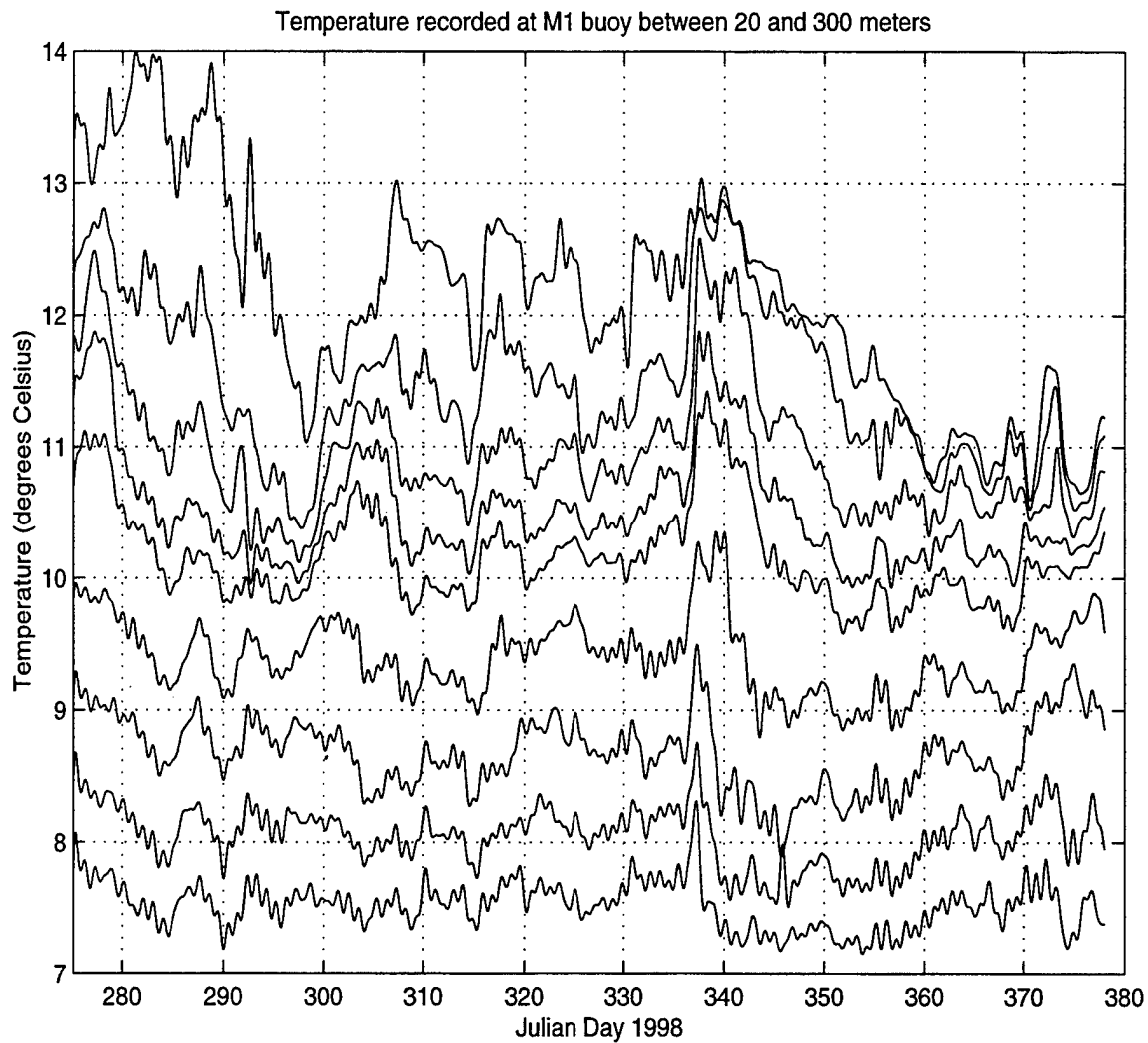


**Fig. 10 – Moored temperature data from the M1 buoy.**

Two major events are seen in the temperature time-series. The first was a large cooling event starting on approximately JD 275, and the second was a more complex perturbation around JD 340. Consistent with the temperature measurements, both events were also observed by the acoustic data (see Fig. 7). Specifically, the cooling event was detected as an increase in the acoustic travel time, whereas the more complex perturbation showed up as path-dependent changes in the travel time.

### III. MODELING

#### A. ARRIVAL STRUCTURE SYNTHESIS

According to ray theory, the received signal is a sum of many individual arrivals, each traveling along an eigenray that connects the source to the receiver. Mathematically, this ray solution representation can be expressed as

$$r(t) = \sum a_n s(t - t_n) e^{-i(2\pi f_0 t_n + \phi_n)}$$

where  $r(t)$  is the complex envelope of the received signal,  $s(t)$  is the complex envelope of the emitted signal,  $f_0$  is the carrier frequency of the transmission, and  $t_n$ ,  $a_n$  and  $\phi_n$  are, respectively, the time delay, magnitude modification and phase shift of the arrival coming from the  $n^{\text{th}}$  eigenray. Therefore, a prediction of the received signal, i.e., the multipath arrival structure, can be obtained if the eigenrays and the associated wave magnitude, phase and delay parameters are known.

To proceed, a computer program called the Hamiltonian Acoustic Raytracing Program for the Ocean (HARPO) (Jones et al., 1986) was used to trace a fan of rays through the "reference" ocean defined earlier. The sound-speed profile and bathymetry of this reference ocean are shown in Figs. 9 and 2, respectively. Ray launch angles varying from  $-30^\circ$  to  $+15^\circ$  at a very fine increment of a  $0.002^\circ$  were used. Rays with launch angles smaller than  $-30^\circ$  and larger than  $+15^\circ$  tended to steepen significantly and suffered great many bottom interactions. Due to high cumulative bottom losses, these rays were not included in the modeling of the arrival structure.

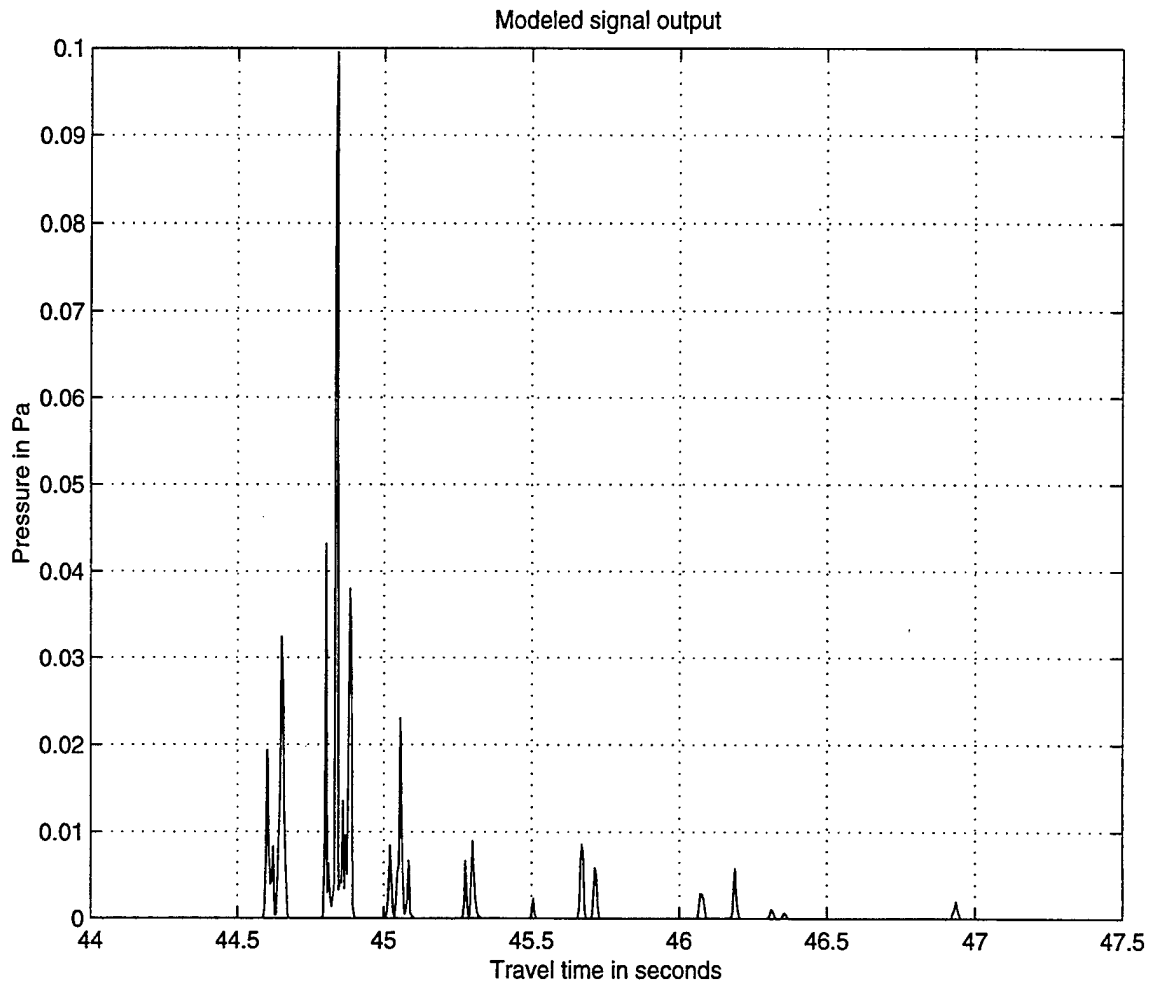


To synthesize the arrival structure, a program called "ray3d" developed by Chiu (1995) was used to process the ray fan computed by HARPO. This program searches for eigenrays, computes travel times to the receiver, calculates all the phase shifts caused by turning points and surface and bottom reflections, and estimates the signal losses due to raytube spreading.

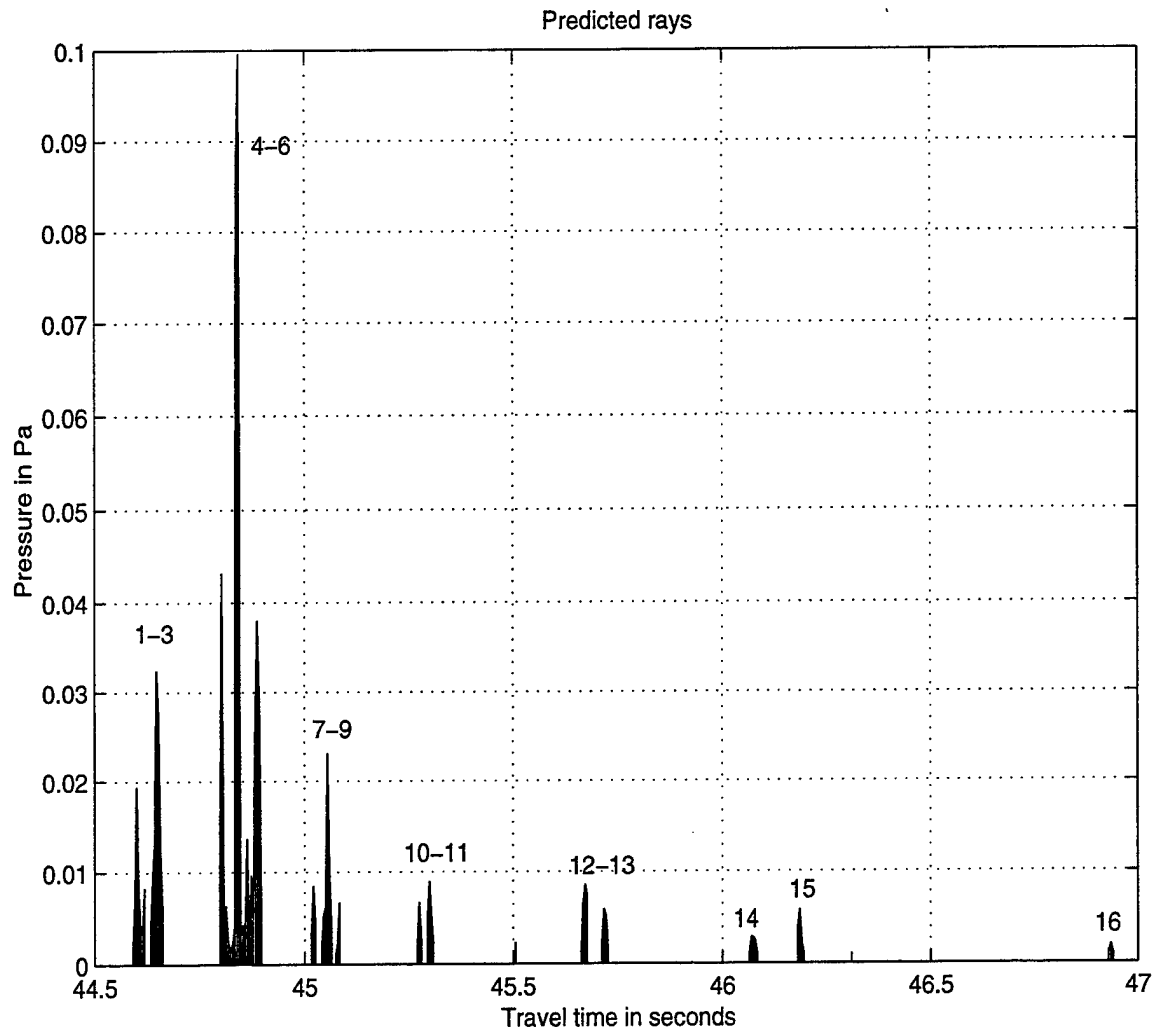
Input sediment information is required by "ray3d" as sediment properties affect both the magnitudes and phases of the ray arrivals through the bottom reflection coefficient. The sediment characteristics between Davidson Seamount and Sur Ridge is variable. In the first half of the path the bottom composition is mainly rock and mud, while closer to Sur Ridge the bottom consists of soft sediment provenient from submarine canyons and underwater landfalls. After some model trials based on a sediment chart and geoacoustic parameter tables (Hamilton, 1972), the best values found to represent the averaged sediment sound speed and sediment density were 1650 m/s and 1600 kg/m<sup>3</sup>, respectively.

Figure 11 shows the magnitude of the modeled complex envelope of the multipath arrival structure, i.e., the output of "ray3d" after processing the HARPO rays. The modeled signal is composed of a total of 166 eigenrays. In order to gain insight into the detailed composition of the signal, the magnitude and travel time associated with each of the 166 individual eigenrays are plotted in Fig. 12 as 166 stems. The stem plot clearly reveals that all of the predicted resolvable arrivals are composed of groups of eigenrays but not individual eigenrays, except for two weak arrivals coming in at approximately 45.5 s and 46.3 s, respectively. Therefore, an outstanding question is: If these group

arrivals were identified in the observed signal, would it be possible to set up accurate forward path-integral relations between sound-speed changes and travel-time changes? This is an important issue affecting the applicability of the tomography inverse technique, and it will be addressed in the next section.



**Fig. 11 – The envelope of the modeled multipath arrival structure.**



**Fig. 12 - A stem plot of the individual eigenray arrivals composing the modeled arrival structure**

To complete the presentation of the ray solution, the geometries of all 166 eigenrays are shown in Fig. 13, whereas the dependence of the travel time to launch angle of the eigenray is displayed in Fig. 14.

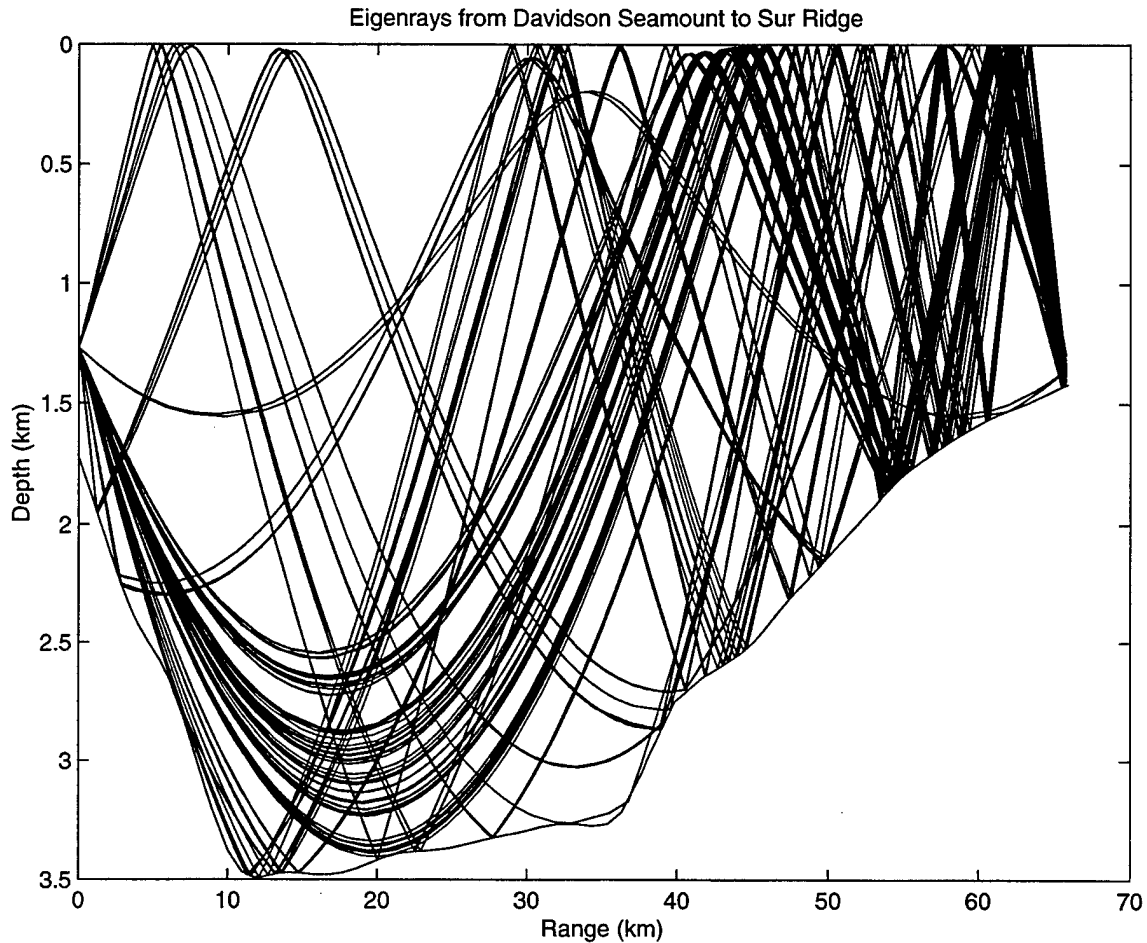


**Fig. 13 – Path geometry's of the eigenrays**

It is easy to see that most of the eigenrays travel downward initially and barely hit the slope of Davidson Seamount. There are a couple of eigenrays that are almost entirely waterborne. The eigenrays that travel upward initially tend to encounter more bottom reflections and hence suffer more energy loss to the bottom. Most of the energy losses occur in the final kilometers of the path close to Sur Ridge where bottom reflections are more frequent. The time-angle information displayed in Fig. 14 helps to understand the order in which the different arrivals come in. The general correspondence of a slower travel time with a steeper ray is shown. This is exactly opposite to the case of a deep

sound channel, but is typical of a bottom-limited coastal channel where the path-length tends to control the gross travel time. A nice grouping behavior of the arrivals is also noticed.

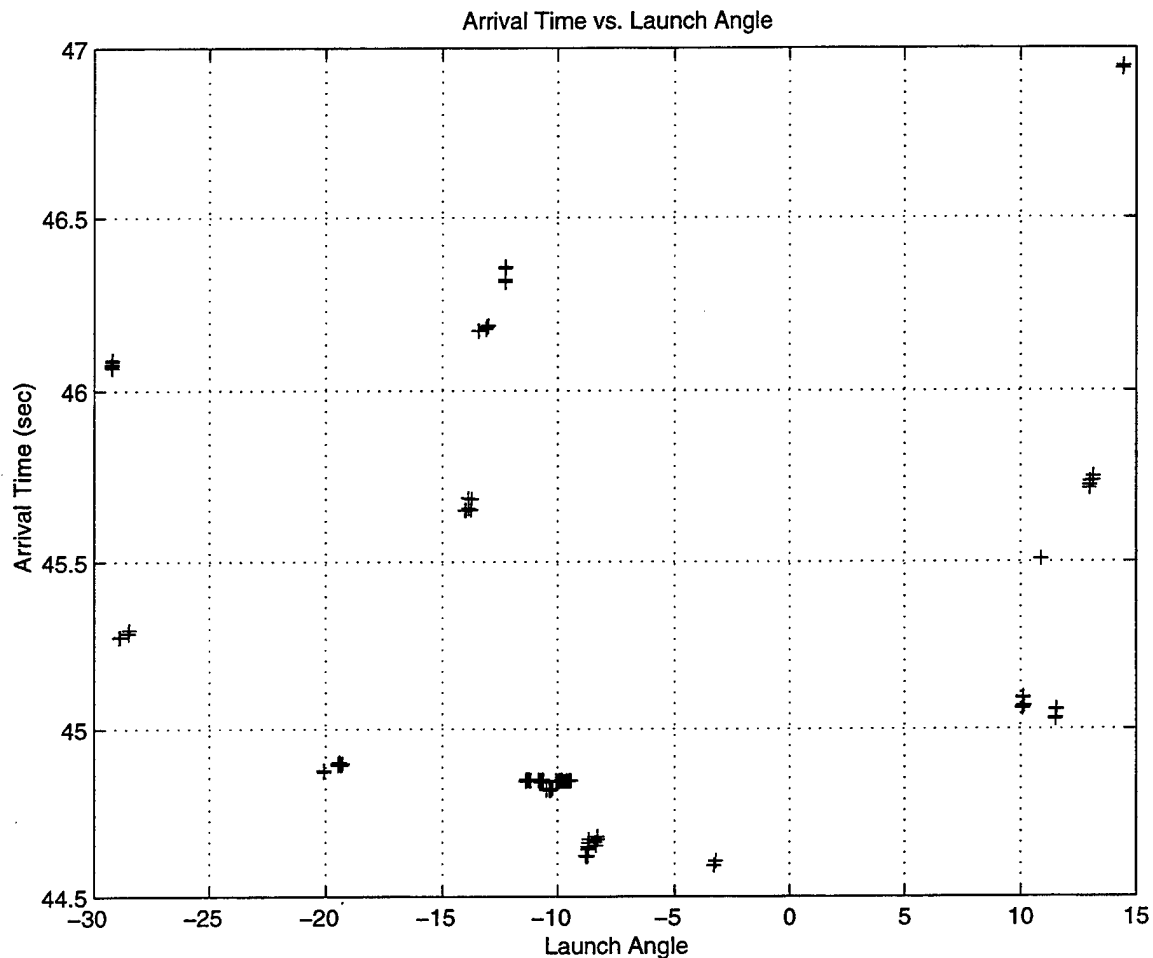


**Fig. 14 – Eigenray travel time versus launch angle**

## **B. RAY IDENTIFICATION**

The identification of the resolved arrivals can be accomplished by comparing the observed arrival structure (Figs. 4 and 6) to the predicted (i.e., modeled) arrival structure (Fig. 12). The resemblance between the observed and predicted is excellent, with 16 group arrivals clearly identified. These 16 group arrivals are labeled by their assigned

identification number from 1 through 16 in Fig. 12. Only two of the predicted arrivals are not observed in the data. The two correspond to extremely weak individual ray arrivals which might have been masked by ambient noise.

To answer the important question of whether one can "invert" the measured travel time series of these group arrivals, the eigenrays associated with each of the 16 groups were isolated. The 16 groups of eigenrays are displayed in Figs. 15 and 16, respectively. With only one exception, the eigenrays of each group are seen to sample essentially the same areas of the ocean. Therefore, it is an accurate approximation to use the mean path of each group to set up the forward path-integral relations between travel time changes and sound-speed changes. The exception is Group 5 which is seen to span different areas.

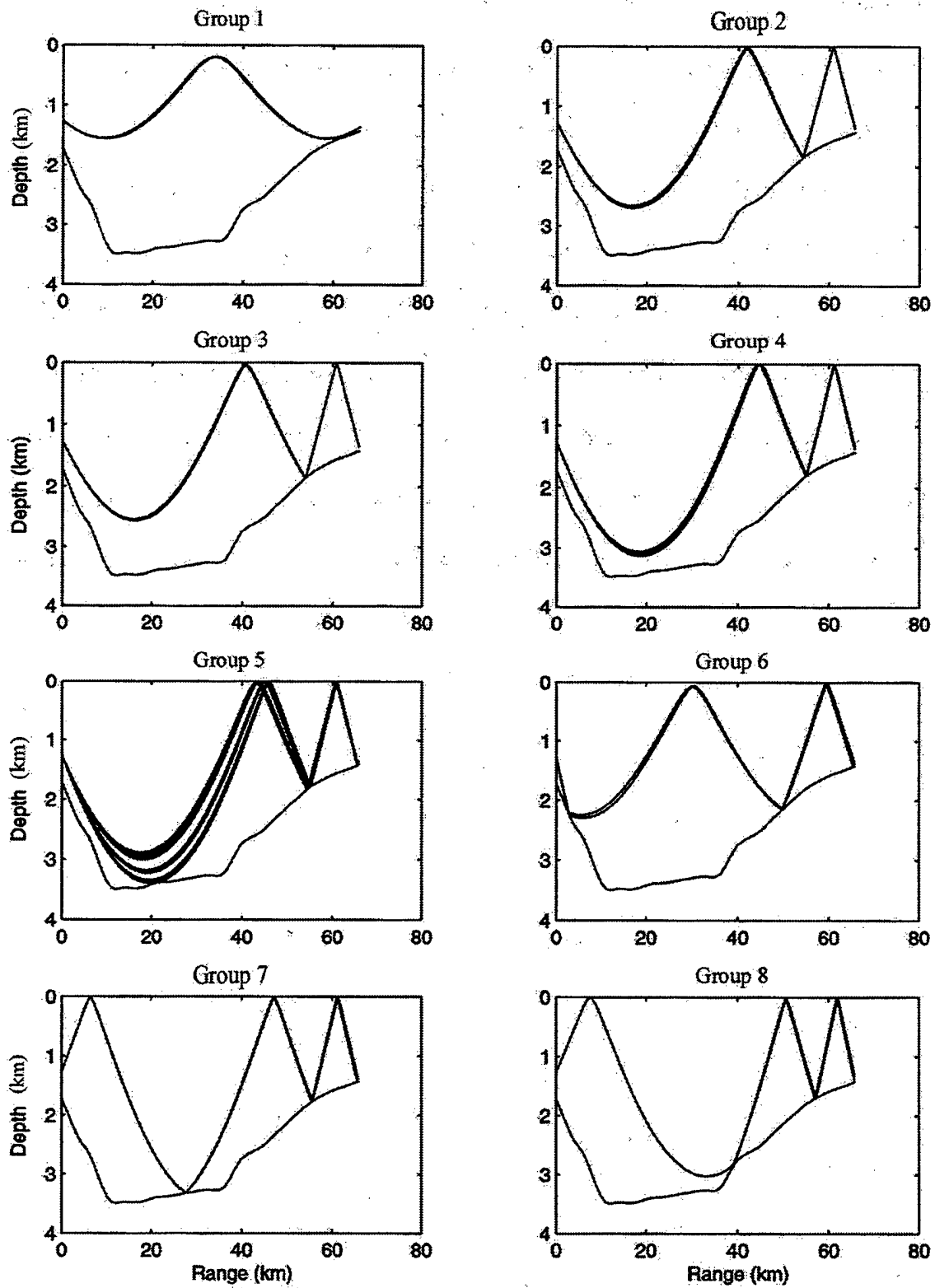


**Fig. 15 – Paths of the eigenray groups 1 to 8**

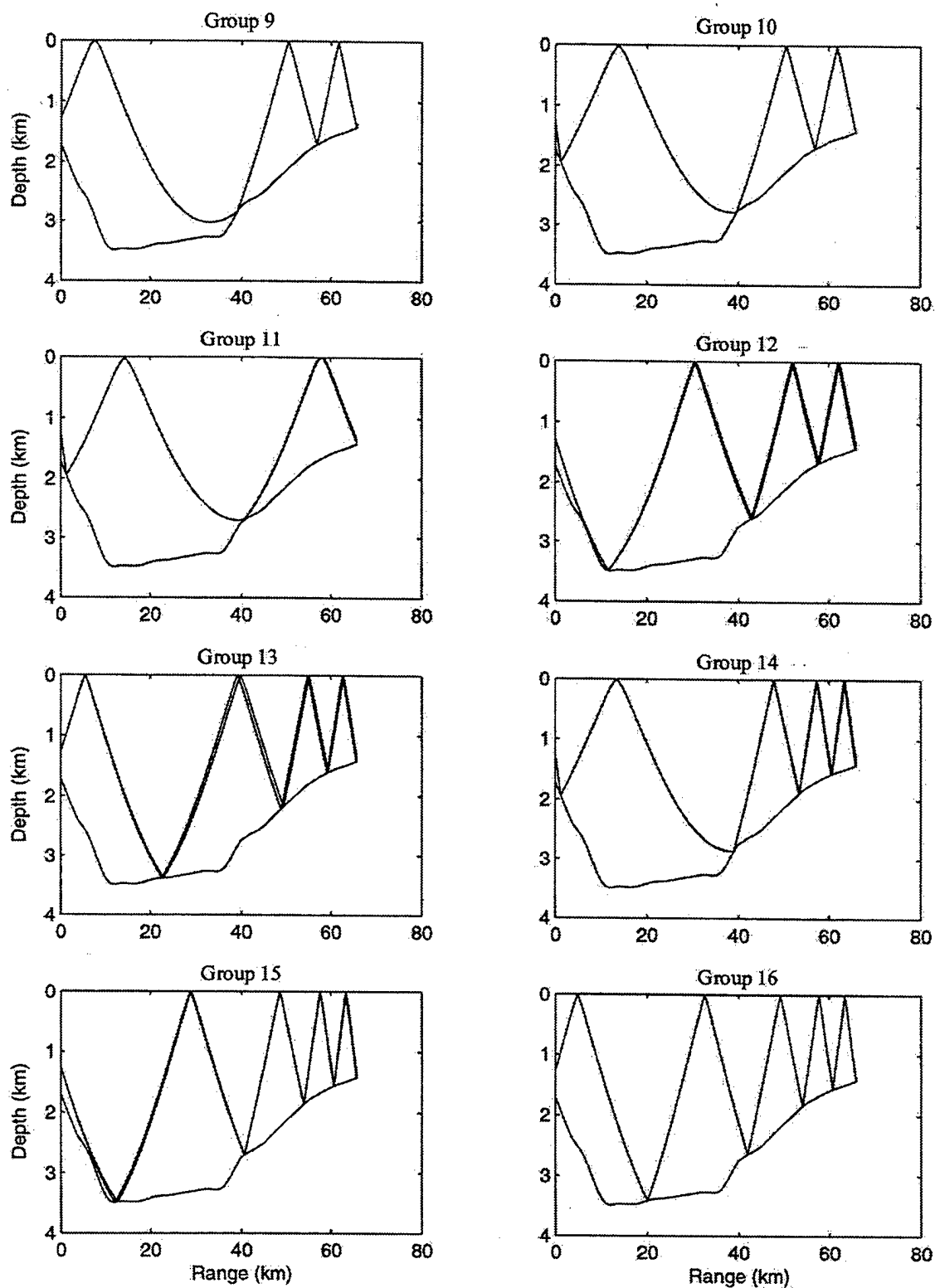


**Fig. 16 – Paths of the eigenray groups 9 to 16**





## IV. VARIABILITY

### A. POWER SPECTRAL DENSITY OF TRAVEL TIME

One of the most important elements in this study was to examine the oceanographic information content in the acoustic travel-time data. The examination was accomplished by constructing power spectral density estimates using the measured travel time series. These spectral estimates help to reveal the dominant ocean oscillations that are sensed by the acoustics and quantify the distribution of signal and noise variances in the data.

The power spectral density functions were estimated using ensemble averages of the squares of the magnitudes of discrete Fourier transforms of non-overlapping segments in the travel time series, and were scaled to give the proper units of  $s^2/cpd$ . A total of 16 power spectral densities were constructed, each gives the distribution of the total variance of the travel time of an arrival in the frequency domain. Each power spectral density is made up of two curves, one covering the higher-frequency portion and the other one the low-frequency portion. The two curves were derived from the data associated with the 30-min and 12-hr transmission intervals, respectively, and they overlap in mid frequencies.

One of these travel-time power spectral densities is displayed in Fig. 17, showing significant peaks around the 12-hr, 24-hr, 8-day, 18-day and 26-day periods. These prominent periods of oscillations persist in almost all 16 travel time series, with few exceptions. To show this, only peaks in the travel-time spectral density are plotted in

Fig.18 for all 16 (group) arrivals. Note that some peaks are missing in some of the spectral densities. Since the 16 groups of eigenrays do sample the ocean differently, it is expected that some are more sensitive or less sensitive to certain types of variability, depending on the associated spatial structures. This is how tomography works.

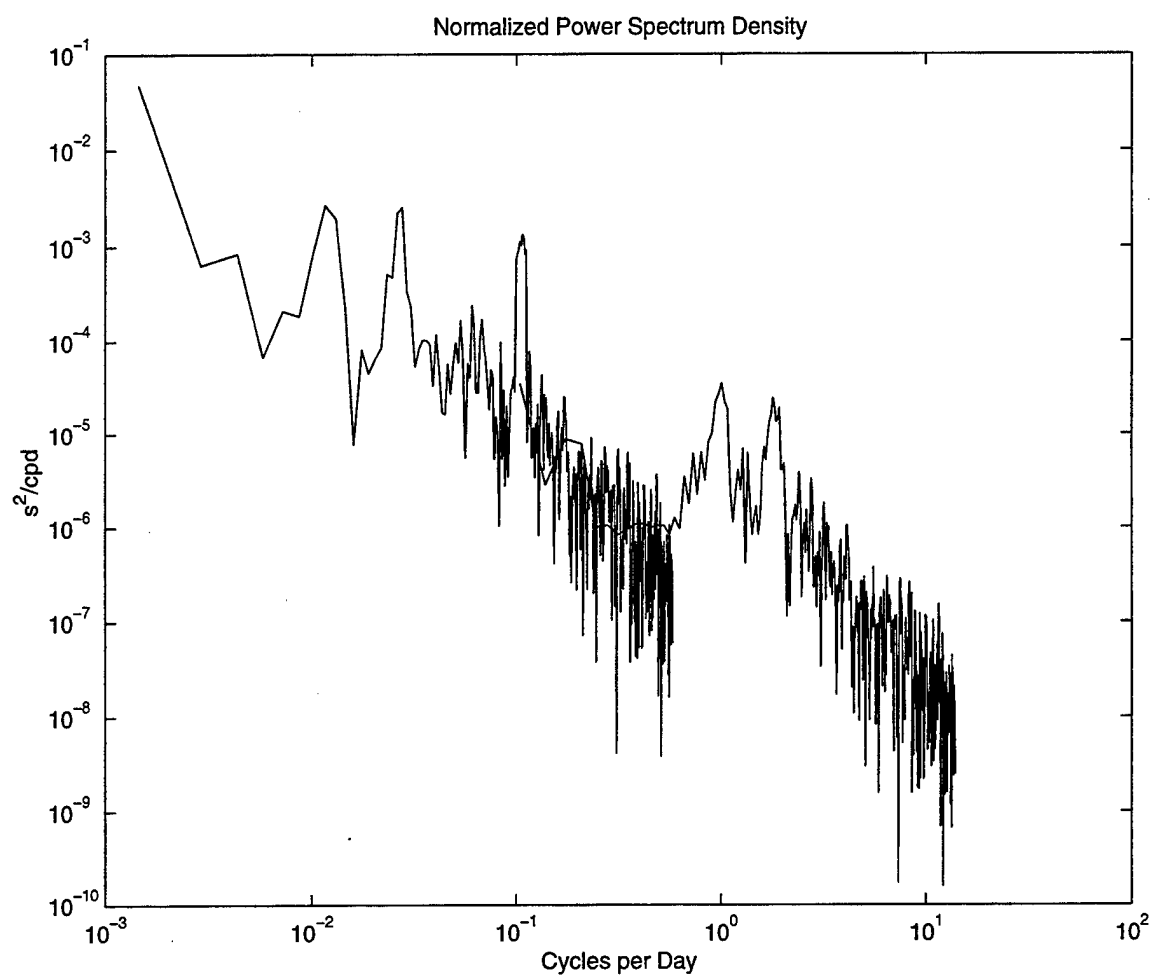


**Fig. 17 – The power spectral density of travel time of one of the group arrivals.**

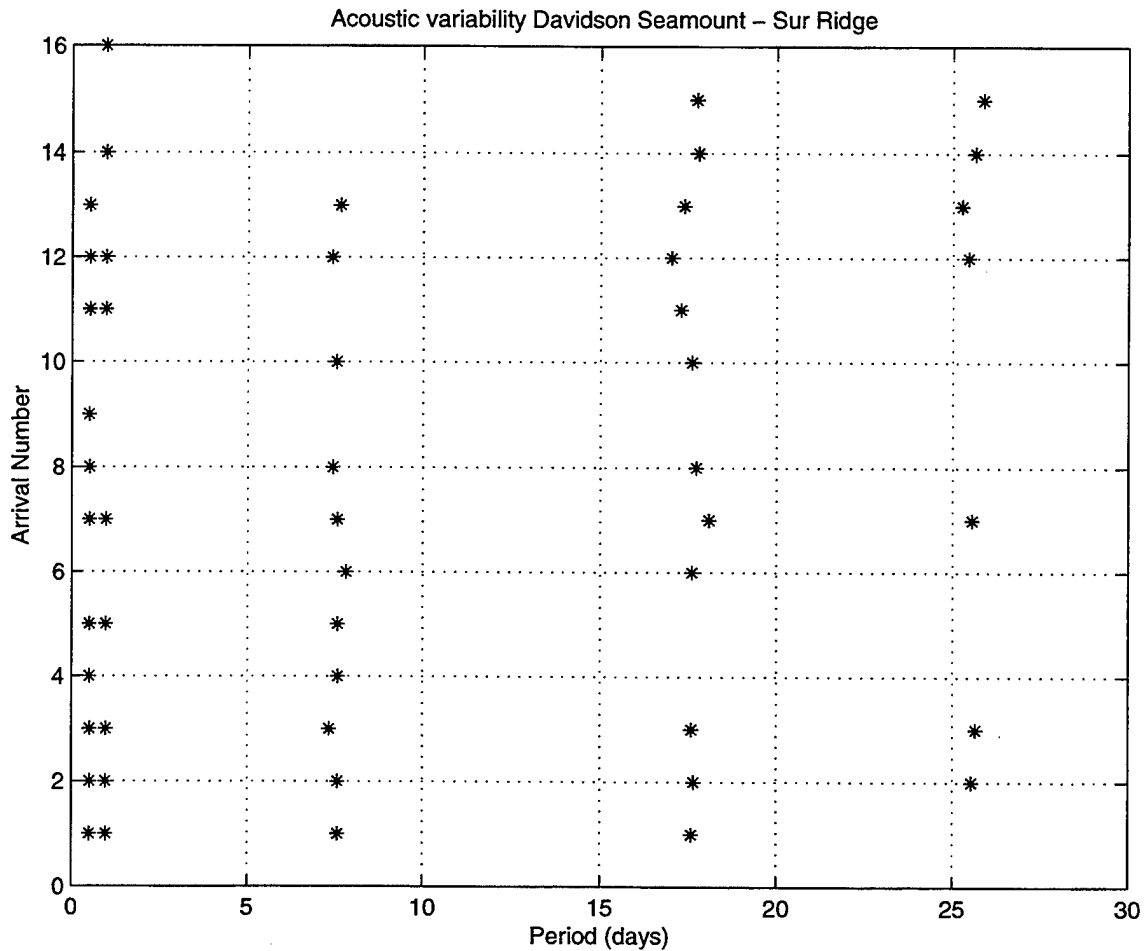


**Fig. 18 – Observed spectral peaks and their corresponding periods.**

The travel-time variations with periods of 12 and 24 hours were caused by semi-diurnal and diurnal tides in the region. The causes of the 8, 18 and 26-day periods are not well understood at this time, however, these same periods were found in the CalCOFI experiment by Collins et al. (1996), who reported notable oscillations with 8 and 18-day periods in the ocean currents and a 26-day period in the ocean temperature. This consistency provides for another confirmation that the travel time data is of high quality.

## B. VARIANCE DISTRIBUTION

Using the power spectral densities, the travel-time variances associated with each of the five prominent periods of oscillations were estimated as the area under the corresponding frequency band. The results are summarized in Table 2, showing that a larger period generally has a larger variance. This is a very desirable outcome in regard to the prospect of long-term ocean monitoring of the synoptic and larger scales using tomography. The tidal variances, in this case, are "noise," which are seen to be considerably smaller than those of the longer scales in general.

However, it is interesting to note that the first arrival measured an exceptionally large variance in the semi-diurnal band. Since the corresponding group of eigenrays never interact with the sea surface, this large travel-time variance was not caused by barotropic tides. The only plausible cause at this frequency band is internal tides. One man's "noise" is another man's "signal." An implication is that tomography transmissions, when performed roughly hourly, could potentially be used to study internal tides in the region.

It can be shown that travel-time variance is directly related to the variance of path-averaged temperature. The relation, to a good approximation, is given by

$$\langle \delta t^2 \rangle = \left( 4.6 * \frac{S}{c^2} \right)^2 \langle \Delta T^2 \rangle$$

where  $\langle \delta t^2 \rangle$  is the variance of travel time,  $S$  the arclength of the raypath,  $c$  the average sound speed, and  $\langle \Delta T^2 \rangle$  the variance of the path-averaged temperature. Using this formula, the results shown in Table 2 were converted into variances of path-averaged temperature. The converted numbers are shown in Table 3. One of the objectives of the

ICON project is the integration of data into a cohesive picture of the coastal environment via a nested, high resolution numerical model. The numbers shown in Table 3 represent measurements of the variances of spatially averaged temperature and are a unique data set for checking the statistics of the ocean model in the validation phase.

		Period of the Variability				
		Semi-diurnal	Diurnal	8 Days	18 Days	26 Days
Arrival Number	1	16.81 ms <sup>2</sup>	3.24 ms <sup>2</sup>	4.41 ms <sup>2</sup>	10.24 ms <sup>2</sup>	---
	2	9.0 ms <sup>2</sup>	4.84 ms <sup>2</sup>	5.29 ms <sup>2</sup>	9.61 ms <sup>2</sup>	27.04 ms <sup>2</sup>
	3	6.76 ms <sup>2</sup>	4.41 ms <sup>2</sup>	4.84 ms <sup>2</sup>	9.0 ms <sup>2</sup>	25.0 ms <sup>2</sup>
	4	2.25 ms <sup>2</sup>	---	5.29 ms <sup>2</sup>	---	---
	5	1.96 ms <sup>2</sup>	1.21 ms <sup>2</sup>	5.76 ms <sup>2</sup>	---	---
	6	---	---	5.29 ms <sup>2</sup>	9.0 ms <sup>2</sup>	---
	7	2.56 ms <sup>2</sup>	1.44 ms <sup>2</sup>	4.84 ms <sup>2</sup>	10.89 ms <sup>2</sup>	25.0 ms <sup>2</sup>
	8	4.0 ms <sup>2</sup>	---	6.76 ms <sup>2</sup>	8.41 ms <sup>2</sup>	---
	9	1.96 ms <sup>2</sup>	---	---	---	---
	10	---	---	7.29 ms <sup>2</sup>	11.56 ms <sup>2</sup>	---
	11	1.0 ms <sup>2</sup>	1.0 ms <sup>2</sup>	---	11.56 ms <sup>2</sup>	---
	12	1.69 ms <sup>2</sup>	1.96 ms <sup>2</sup>	5.29 ms <sup>2</sup>	8.41 ms <sup>2</sup>	18.49 ms <sup>2</sup>
	13	1.44 ms <sup>2</sup>	---	3.24 ms <sup>2</sup>	4.41 ms <sup>2</sup>	12.25 ms <sup>2</sup>
	14	---	1.44 ms <sup>2</sup>	---	6.25 ms <sup>2</sup>	18.49 ms <sup>2</sup>
	15	---	---	---	6.25 ms <sup>2</sup>	25.0 ms <sup>2</sup>
	16	---	1.0 ms <sup>2</sup>	---	---	---

**Table 2 – Travel Time Variance Distribution**

		Period of the Variability				
		Semi-diurnal	Diurnal	8 Days	18 Days	26 Days
Arrival Number	1	0.89 C <sup>2</sup>	0.18 C <sup>2</sup>	0.24 C <sup>2</sup>	0.56 C <sup>2</sup>	---
	2	0.44 C <sup>2</sup>	0.24 C <sup>2</sup>	0.25 C <sup>2</sup>	0.49 C <sup>2</sup>	1.37 C <sup>2</sup>
	3	0.33 C <sup>2</sup>	0.22 C <sup>2</sup>	0.24 C <sup>2</sup>	0.45 C <sup>2</sup>	1.27 C <sup>2</sup>
	4	0.11 C <sup>2</sup>	---	0.27 C <sup>2</sup>	---	---
	5	0.09 C <sup>2</sup>	0.06 C <sup>2</sup>	0.28 C <sup>2</sup>	---	---
	6	---	---	0.27 C <sup>2</sup>	0.46 C <sup>2</sup>	---
	7	0.12 C <sup>2</sup>	0.08 C <sup>2</sup>	0.23 C <sup>2</sup>	0.54 C <sup>2</sup>	1.22 C <sup>2</sup>
	8	0.18 C <sup>2</sup>	---	0.33 C <sup>2</sup>	0.42 C <sup>2</sup>	---
	9	0.09 C <sup>2</sup>	---	---	---	---
	10	---	---	0.35 C <sup>2</sup>	0.56 C <sup>2</sup>	---
	11	0.05 C <sup>2</sup>	0.05 C <sup>2</sup>	---	0.59 C <sup>2</sup>	---
	12	0.08 C <sup>2</sup>	0.09 C <sup>2</sup>	0.24 C <sup>2</sup>	0.40 C <sup>2</sup>	0.92 C <sup>2</sup>
	13	0.06 C <sup>2</sup>	---	0.15 C <sup>2</sup>	0.20 C <sup>2</sup>	0.58 C <sup>2</sup>
	14	---	0.07 C <sup>2</sup>	---	0.28 C <sup>2</sup>	0.87 C <sup>2</sup>
	15	---	---	---	0.27 C <sup>2</sup>	1.15 C <sup>2</sup>
	16	---	0.05 C <sup>2</sup>	---	---	---

**Table 3 – Variances of path-averaged temperature.**

## V. CONCLUSIONS

The repeated transmissions of a tomography signal from an autonomous sound source placed on Davidson Seamount are continuously monitored by a bottom-lying receiver on Sur Ridge. The received analog signals are transmitted back to the NPS OAO via an underwater telecommunication cable where they are digitized and archived.

To address the signal stability, resolvability and identifiability criteria that determine the applicability of ocean tomography along this path, the data recorded from July 1998 to January 1999 were first processed to obtain the multipath pulse arrival structure and its variability in time. A signal processing lesson was learned: A rate slightly above the theoretical Nyquist criterion (i.e., twice the transmission frequency) was shown to be insufficient to produce an improved SNR through coherent averaging of the consecutive signal sequences. An aliasing effect, corresponding to the introduction of a frequency-independent phase roll in the digitized signal, was found. However, a sufficient SNR gain can still be realized using incoherent averaging. No aliasing effects were found when digitized at five times the transmission frequency.

The processed signals show strong arrivals that are both stable and resolvable. In order to identify the resolved arrivals, acoustic propagation modeling was performed using ray theory in conjunction with measured sound speed and high-resolution bathymetric data. A comparison of the predicted and measured arrival structures show that the observed arrivals are clearly identifiable and are made up of eigenray groups (i.e., eigenray tubes) instead of individual eigenrays. Since the eigenrays within each group



(except for only one group) are found to have almost identical trajectories through the ocean, the common passage along which the ray group integrates the ocean variability is unambiguous.

Consistent with previous CalCOFI observations (Collins et al., 1996), the extracted ray group travel time series exhibit dominant oscillations with semidiurnal, diurnal, 8-day, 18-day and 26-day periods, respectively. Using spectral estimation techniques, the travel time variances of these dominant oscillations were quantified. These travel time variances represent direct measurements of the variances of spatially averaged ocean temperatures. Therefore, not only are they useful for establishing the solution and noise variances for the construction of the inverse solution, they also constitute a powerful statistical data set for the validation of ocean models for the region.

## LIST OF REFERENCES

- Chelton, D.B., "Seasonal Variability of Along Shelf Geostrophic Velocity off Central California," *J. Phys. Oceanogr.*, 12, pp 757-784, 1984.
- Chiu, C.-S., A.J. Semtner, C.M. Ort, J.H. Miller, and L.L. Ehret, "A Ray Variability Analysis of Sound Transmissions from Heard Island to California," *The Journal of the Acoustic Society of America*, Vol. 96(4), pp 2380-2388, 1994.
- Chiu, C.-S., J.H. Miller and J.F. Lynch, "Inverse Techniques for Coastal Acoustic Tomography," in *Environmental Acoustics*, D. Lee and M. Schultz, Eds., World Scientific, 1994 a.
- Collins, C.A., N. Garfield, R.G. Paquette, and E.Carter, "Lagrangian Measurements of Subsurface Poleward Flow Between 38°N and 43°N Along the West Coast of The United States During Summer, 1993," *Geophys. Res. Lett.*, 23(18), pp 2461-2464, 1996.
- Collins, C.A., R.G. Paquette, and S.R. Ramp, "Annual Variability of Ocean Currents at 350-M Depth over the Continental Slope off Point Sur, California," *CalCOFI Rep.*, Vol. 37, pp 257-263, 1996.
- Cornuelle, B.D., "Inverse Methods and Results From the 1981 Ocean Acoustic Tomography Experiment", Ph.D. Thesis, Massachusetts Institute of Technology – Woods Hole Oceanographic Institution Joint Program in Oceanography, 1983.
- Hamilton, E.L., "Compressional-Wave Attenuation in Marine Sediments," *Geophysics*, Volume 37(4), pp 620-646, 1972.
- Hickey, B.M., "Coastal Oceanography of Western North America From the Tip of Baja California to Vancouver Island," *The Sea*, Volume 11, pp 345-393, 1998.
- Hickey, B.M., "The California Current System: Hypothesis and Facts," *Prog. Oceanogr.*, 8, pp 191-279, 1979.
- Huyer, A., and R.L. Smith, "A Subsurface Ribbon of Cool Water Over the Continental Shelf off Oregon," *J. Phys. Oceanogr.*, 4, pp 381-391, 1974.
- Jones, R.M., J.P. Riley, and T.M. Georges, "HARPO: A Versatile Three-Dimensional Hamiltonian Ray Tracing Program for Acoustic Waves in Ocean with Irregular Bottom," *Wave Propagation Laboratory, National Oceanic and Atmospheric Administration, Boulder, CO*, 457 pp., 1986.

Monterey Bay Aquarium Research Institute (MBARI), <http://www.mbari.org>, Moss Landing, CA.

Morvillez, T., "Monitoring Temperature Variability Along the California Coast Using Acoustic Tomography," Master's Thesis, Naval Postgraduate School – Monterey, CA, September 1997.

Munk, W., P. Worcester, and C. Wunsch, "Ocean Acoustic Tomography," Cambridge University Press, New-York, 1995.

Pavlova, Y.V., "Seasonal Variations of the California Current," *Oceanology*, 6, pp 806-814, 1966

Rosenfeld, L.K., F.B. Schwing, N. Garfield, and D. Tracy, "Bifurcated Flow from an Upwelling Center: a Cold Water Source for Monterey Bay," *Cont. Shelf Res.*, 14(9), pp 931-964, 1994.

Tisch, T.D., S.R. Ramp, and C.A. Collins, "Observations of the Geostrophic Current and Water Mass Characteristics off Point Sur, California, from May 1988 through November 1989," *J. Geophys. Res.* 97(C8), pp 12535-12556, 1992.

Wooster, W.S., and J.H. Jones, "The California Undercurrent off Baja California," *J. Mar. Res.*, 28(2), pp 235-250, 1970.

## INITIAL DISTRIBUTION LIST

	No. Copies
1. Defense Technical Information Center..... 8725 John J. Kingman Rd., STE 0944 Ft. Belvoir, Virginia 22060-6218	2
2. Dudley Knox Library..... Naval Postgraduate School 411 Dyer Rd. Monterey, California 93943-5101	2
3. Dr. Roland W. Garwood Jr., OC/Co..... Oceanography Department Naval Postgraduate School 883 Dyer Rd., RM 324 Monterey, CA 93943-5122	1
4. Dr. Ching-Sang Chiu, OC/Ci..... Oceanography Department Naval Postgraduate School 883 Dyer Rd., RM 324 Monterey, CA 93943-5122	2
5. Dr. Curtis Collins, OC/Co..... Oceanography Department Naval Postgraduate School 883 Dyer Rd., RM 324 Monterey, CA 93943-5122	2
6. Mr. Chris Miller..... Naval Postgraduate School 589 Dyer Rd., RM 200A Monterey, CA 93943-5143	1
7. Embassy of Portugal..... Naval Attache 2310 Tracy Place, N.W. Washington, D.C. 20008	2
8. Dr. Steve Ramp (Code OC/Ra)..... Department of Oceanography Naval Postgraduate School 833 Dyer Rd., RM 324 Monterey, CA 93943-5122	1

9. Dr. Jeffrey Paduan (Code OC/Pd).....1  
Department of Oceanography  
Naval Postgraduate School  
833 Dyer Rd., RM 324  
Monterey, CA 93943-5122
  
10. Dr. Leslie Rosenfeld (Code OC/Ro).....1  
Department of Oceanography  
Naval Postgraduate School  
833 Dyer Rd., RM 324  
Monterey, CA 93943-5122
  
11. Dr. Francisco Chavez.....1  
Monterey Bay Aquarium Research Institute  
P.O. Box 628  
Moss Landing, CA 95039-0628
  
12. Cynthia Decker.....1  
National Ocean Partnership Program  
1755 Massachusetts Ave. N.W.  
Washington, D.C. 20036-2102
  
13. CDR Richard Barock, N874C.....1  
Office of the Chief of Naval Operations  
2000 Navy Pentagon  
Washington, DC 20350-200
  
14. Dr. Jeff Simmen.....1  
Office of Naval Research  
800 North Quincy Street  
Arlington, VA 22217
  
15. Director Geral do Instituto Hidrografico.....2  
Instituto Hidrografico  
Rua das Trinas, 49  
1296 LISBOA CODEX  
Portugal
  
16. LT Jose Alberto de Mesquita Onofre.....2  
Instituto Hidrografico  
Rua das Trinas,49  
1296 LISBOA CODEX  
Portugal